Accepted Manuscript

Control of mercury and methylmercury in contaminated sediments using biochars: A long-term microcosm study

Peng Liu, Carol J. Ptacek, David W. Blowes, W. Douglas Gould

PII: S0883-2927(18)30042-8

DOI: 10.1016/j.apgeochem.2018.02.004

Reference: AG 4040

To appear in: *Applied Geochemistry*

Received Date: 20 September 2017

Revised Date: 7 February 2018

Accepted Date: 13 February 2018

Please cite this article as: Liu, P., Ptacek, C.J., Blowes, D.W., Gould, W.D., Control of mercury and methylmercury in contaminated sediments using biochars: A long-term microcosm study, *Applied Geochemistry* (2018), doi: 10.1016/j.apgeochem.2018.02.004.

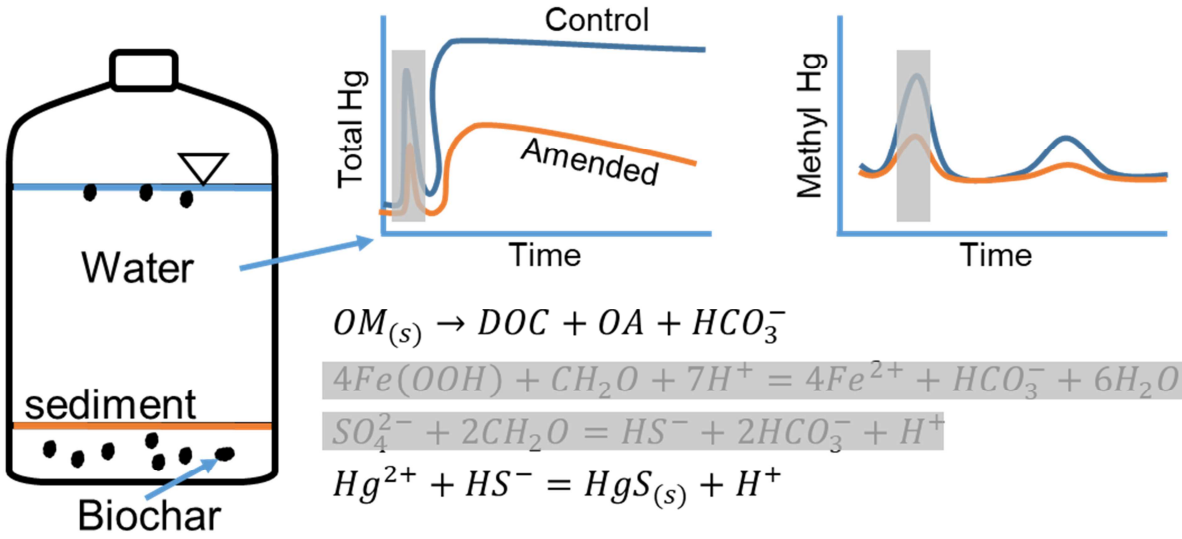

$$OM_{(s)} \rightarrow DOC + OA + HCO_3^-$$

$$4Fe(OOH) + CH_2O + 7H^+ = 4Fe^{2+} + HCO_3^- + 6H_2O$$

$$SO_4^{2-} + 2CH_2O = HS^- + 2HCO_3^- + H^+$$

$$Hg^{2+} + HS^- = HgS_{(s)} + H^+$$

$$CH_3^- + Hg^{2+} = CH_3Hg^+$$

Control of mercury and methylmercury in contaminated sediments using biochars: a long-term microcosm study

Peng Liu[a,b], Carol J. Ptacek[*,b], David W. Blowes[b], W. Douglas Gould[b]

[a]*School of Environmental Studies, China University of Geosciences, 388 Lumo Rd., Wuhan, Hubei, 430074, P. R. China*
[b]*Department of Earth and Environmental Sciences, University of Waterloo, 200 University Ave. W., Waterloo, ON, Canada N2L 3G1*

[*] Corresponding author address: Department of Earth and Environmental Sciences, University of Waterloo, 200 University Ave. W., Waterloo, ON, Canada N2L 3G1. Tel: +01 (519) 888 4567, ext. 32230
E-mail: ptacek@uwaterloo.ca

Abstract

The effectiveness of activated carbon and four types of biochar, switchgrass (300 °C and 600 °C), poultry manure (600 °C), and oak (~700 °C) with respect to mercury (Hg) and methylmercury (MeHg) control was assessed in microcosm experiments carried out for 524 d. Early in the study (<30 d), minimal differences in concentrations of <0.45-µm filtered total Hg (THg) in control and 5% biochar-amended systems were observed. At later stages, THg concentrations in the amended systems decreased to 8-80% of concentrations in the sediment controls. Aqueous concentrations of MeHg were generally lower in the amended systems than in the controls, with an initial peak in MeHg concentration corresponding to the onset of iron and sulfate reduction (~40 d) and a second peak to methanogenic conditions (~400 d). Pyrosequencing analyses indicate the microbial communities initially associated with fermenters and later shifted to iron-reducing bacteria (FeRB), sulfate-reducing bacteria (SRB), and methanogens. These analyses also indicated the existence of 12 organisms associated with Hg methylation in all systems. Community shifts were correlated with changes in the concentrations of carbon sources (dissolved organic carbon (DOC) and organic acids) and electron acceptors (NO_3^-, Fe, and SO_4^{2-}). Co-blending of biochars with Hg-contaminated sediment is an alternative remediation method for controlling the release of Hg and MeHg.

Key words: Mercury; Methylmercury; Biochar; Sediment; Remediation; Geochemistry

1 Introduction

A number of industrial activities, including coal combustion (Yudovich and Ketris, 2005), refuse incineration (Cheng and Hu, 2012), and Au and Hg mining (Mendes et al., 2016), have resulted in release of Hg and widespread contamination of receiving watersheds. In

such watersheds, Hg is often unevenly distributed within sediments, soils, and groundwater and readily cycled among different phases (Jackson, 2016). . Methylmercury (MeHg), an organic form of Hg, is much more bioaccumulative and toxic than Hg in inorganic forms (Clarkson and Magos, 2006; Tchounwou et al., 2003). Methods such as sediment dredging (Han et al., 2006) and *in situ* amendment (Ahmad et al., 2014; Gilmour et al., 2013; Hilber and Bucheli, 2010; Liu et al., 2017; Patmont et al., 2015; Serrano et al., 2012) are available for the remediation of Hg-contaminated sites (Mulligan et al., 2001; Randall and Chattopadhyay, 2013),

MeHg is primarily produced through biotic processes under reducing conditions. The organisms, which can methylate Hg, mainly include sulfate-reducing bacteria (SRB) (Gilmour et al., 1992), iron reducing bacteria (FeRB) (Kerin et al., 2006; Yu et al., 2011), and methanogens (Hamelin et al., 2011; Yu et al., 2013). These organisms utilize various carbon sources and electron acceptors (Fe(III) and SO_4^{2-}) to methylate bioavailable Hg. Adsorbents can be applied to remove MeHg and Hg directly from the aqueous phase to minimize mass transport (Gomez-Eyles et al., 2013). Another method to control MeHg is the diminution of Hg bioavailability through its conversion to chemically stable forms (Wang et al., 2012).

Different reactive materials are available for stabilizing Hg, including activated carbon (AC) (Gilmour et al., 2013; Hilber and Bucheli, 2010; Patmont et al., 2015), zero-valent Fe (Weisener et al., 2005), sulfurized clay (Gibson et al., 2011), sulfate-type cements (Serrano et al., 2012; Serrano et al., 2016), sulfur and iron (Zhong et al., 2018), and biochars (Ahmad et al., 2014; Li et al., 2017; Liu et al., 2016). However, most of the reactive materials are expensive and not practical for large contaminated sites, resulting

in the need to identify cost-effective materials to control Hg for remediation of large areas.

Pyrolyzed carbon, including AC and biochars derived from a range of plant materials, has been applied to reduce Hg or MeHg bioaccumulation or concentrations in pore water in sediment (Bundschuh et al., 2015; Gilmour et al., 2013; Gomez-Eyles et al., 2013; Huntington et al., 2015). In Gilmour et al. (2013) and Gomez-Eyles et al. (2013), pore water concentrations and bioaccumulation of Hg and MeHg were effectively reduced in freshwater sediment amended with AC; biochar was effective for MeHg sorption but less effective for control of inorganic Hg. These two studies were conducted for 15 d and focused on bioaccumulation and distribution of Hg and MeHg between the aqueous and solid phase (Gilmour et al., 2013; Gomez-Eyles et al., 2013). Bundschuh et al. (2015) report Hg bioaccumulation decreased after amending sediments with pyrolyzed carbon for up to 175 d. Huntington et al. (2015) report the application of AC decreases pore water MeHg concentration, but not MeHg content, in sediments in field mesocosms operated for 91 d. The decrease of MeHg concentration in pore water was attributed to adsorption by AC.

The studies that used pyrolyzed carbon to treat Hg-contaminated sediment focused on the bioaccumulation of Hg or MeHg; most concentration decreases were attributed to adsorption, and the experimental period was relatively short (15 or up to 175 d). Sediments are often rich in organic matter and can contain various Fe- and sulfate-containing minerals. DOC, labile organic carbon, alkalinity (carbon source for methanogens), and SO_4^{2-} are released from various biochars and AC (Liu et al., 2015; Liu et al., 2016; Riedel et al., 2014; Uchimiya et al., 2013). All of these components might

affect Hg speciation and MeHg evolution upon application of pyrolyzed carbon to the sediment. For example, potential Hg methylators can methylate Hg by utilizing labile carbon as an energy source (electron donor) and Fe and SO_4^{2-} as electron acceptors, biogenic S^{2-} and Hg combine to form Hg-S precipitates, Fe(II) formed from the reduction of Fe(III) and dissolved Hg compete for S^{2-}, and dissolved organic matter (DOM) and Hg form Hg-DOM complexes.

This study evaluated the stabilization of Hg and MeHg using AC and four distinct biochars over an extended period of time (>500 d). Microcosm experiments were conducted in an anaerobic chamber by mixing sediment, biochars, and water. Liu et al. (2017) report the stabilization of Hg using two of the four biochars (switchgrass biochars pyrolyzed at 300 and 600 °C). The present study complements this previous work by evaluating the control of Hg and MeHg using more biochar samples and discussing in depth the factors that affect control of Hg and MeHg. Geochemical measurements and pyrosequencing analyses were conducted to track shifts in the microbial community with time and provide insights into mechanisms controlling Hg and MeHg evolution after amending with biochars.

2 Materials and Methods

2.1 Materials

Sediment was collected from an Hg-contaminated site on the South River near Waynesboro, VA, USA, 5.6 km downstream from a historic point of Hg release (Fig. 1). River water was collected upstream (~0.3 km) of the historic release point. Four biochar samples were employed in the study. Feedstocks of the biochars were air-dried and pyrolyzed using a kiln at either 300 or 600 °C for 2-3 h under O_2-deficit conditions. The biochars include switchgrass biochars (300 °C, GRASS300 and 600 °C, GRASS600) and

poultry manure biochar (600 °C, MANURE600) prepared using methods provided in detail by Liu et al. (2015), and commercial oak biochar (rejects of product from Cowboy Charcoal, ~700 °C, OAK700). Commercial AC (Sigma-Aldrich Corp.) was used as a benchmark for comparison.

2.2 Anaerobic Microcosm Experiments

Microcosm experiments were conducted by mixing biochar, sediment, and river water at a ratio of 1:20:160 (mass: 5, 100, and 800 g) in amber glass bottles. Controls included ultra-pure water, river water, sediment mixed with river water, and biochar mixed with river water. The sediment control and OAK700- and MANURE600-amended systems were duplicated to facilitate statistical analysis. The experiments were conducted in an anaerobic chamber (Coy Laboratory Products Inc.) with a gas mixture of 3.5% H_2 balanced N_2. Argon was used to replace the volume removed during sampling events. The amber bottles were shaken thoroughly to remix the solid and aqueous phases after each sampling event.

Aqueous samples were collected throughout the experiment using Norm-Ject syringes (Henke Sass Wolf). Aliquots of 0.45-μm filtered (Pall Corp.) sample were collected for alkalinity, anion, total Hg (THg), MeHg, cation, DOC, and nutrient (NH_3-N and PO_4-P) analyses as well as ultraviolet (UV) absorbance at 254 nm. Because Hg is known to bind to colloids of different sizes (Poissant and Pilote, 1998; Stordal et al., 1996), unfiltered and 0.2-μm filtered samples were also collected for THg analysis. Duplicate sampling events were regularly executed for quality assurance and quality control. Samples for THg, MeHg, and DOC were stored in 15-mL amber vials (VWR International). Samples for anion, cation, and UV analyses were stored in 15-mL high-

density polypropylene (HDPE) bottles (Thermo Scientific). Samples for anion analyses were maintained at 4 °C and analyzed within 48 h. Samples for cation and THg analyses were acidified using 15.6N HNO_3 and stored at 4 °C. Samples for the determination of MeHg (acidified with 12.1N HCl), DOC, nutrients (acidified using 8N H_2SO_4), and UV absorbance (unacidified) were stored at -20 °C. Acidified samples had pH values <2. Solid samples were collected periodically for MeHg and pyrosequencing analyses using a spatula and stored at -20 °C before analysis. The sampling time and methods were the same as presented in Liu et al. (2017).

2.3 Water Analyses

Values of pH, Eh, and alkalinity were determined inside the anaerobic chamber immediately after sample collection. Value of pH was determined on unfiltered samples using a Ross combination pH electrode (Orion 815600, Thermo Scientific), calibrated against pH 4, 7, and 10 buffers. Redox potential (Eh) was determined on unfiltered samples using an electrode (Orion 9678, Thermo Scientific), the performance of which was checked against ZoBell's (Nordstrom, 1977) and Light's (Light, 1972) solutions. The reported value was corrected with the standard hydrogen electrode. Alkalinity was determined by adding bromocresol green-methyl red indicator and titrating to the end point using 0.16 mol L^{-1} H_2SO_4 and a digital titrator (HACH, Loveland).

Concentrations of anions (including short-chain organic acids (OA)) were determined using ion chromatography (ICS-5000, Dionex Corp.) with an IonPac AS11 4×250 mm column. NH_3-N concentrations were determined using the salicylate spectrophotometric method (Hach Test Method 8155). DOC was determined using an automated wet chemical oxidation method (Aurora 1030, OI Analytical). UV absorbance

was measured at 254 nm (UV_{254}) using a UV-visible spectrophotometer (Evolution 260, Thermo Scientific). Specific UV absorbance ($SUVA_{254}$) was expressed as the ratio of absorbance at 254 nm per meter to DOC concentrations.

Cation concentrations were determined by inductively coupled plasma-optical emission spectrometry (ICP-OES; Thermo Scientific iCAP 6500) and inductively coupled plasma-mass spectrometry (ICP-MS; Thermo Scientific XSeries II). NH_3-N concentrations were determined using the salicylate spectrophotometric method (Hach Test Method 8155). PO_4-P concentrations were measured using the ascorbic acid spectrophotometric method (Hach Test Method 8048).

THg was determined using a cold vapor atomic fluorescence spectroscopy technique (CVAFS, Tekran 2600) following EPA method 1631 (US EPA, 2002). The method detection limit (MDL) for THg was 0.2 ng L^{-1} (EPA 0.2 ng L^{-1}; Tekran 0.02 ng L^{-1}) determined following the EPA procedure (40 CFR, Part 136). MeHg was analyzed through distillation (Tekran 2750), aqueous ethylation, and purge and trap with the CVAFS technique (Tekran 2700) following EPA method 1630 (US EPA, 2002). Determination of the MDL for MeHg was performed for each run and an averaged MDL of 0.02 ng L^{-1} was calculated (EPA 0.02 ng L^{-1}; Tekran 0.004 ng L^{-1}). The quality assurance and quality control (QA/QC) of MeHg analysis were presented in Table S1-S3, including method blanks, distillation standard recovery, and detection limit.

2.4 Solid Phase Analysis

Wet solid samples for MeHg analysis were mixed with 20% KCl, 8M H_2SO_4, and $CuSO_4$ for distillation to improve recovery following the method described by Horvat et al.

183 (1993). The distilled aqueous phase was then ethylated and analyzed by CVAFS as
184 described previously for the aqueous MeHg samples.

185 Genomic DNA was isolated and purified from wet solid phase using commercial
186 extraction kits (UltraClean Soil DNA Kit; MO BIO Laboratories) following the
187 supplier's instructions. Purified DNA was stored at -20 °C up to one week and shipped
188 on ice to MR DNA Laboratory (Shallowater, TX) for pyrosequencing analyses. Detailed
189 information on the primers used, the processes and conditions of polymerase chain
190 reaction and sequencing, and data processing procedures is provided in Liu et al. (2017).
191 Databases of fermenters, FeRB, SRB, and methanogens were assembled based on
192 published sources (Table S4-S7). A database of potential Hg methylators was also
193 assembled by Liu et al. (2017) based on the methylators identified by Oak Ridge National
194 Laboratory (2015). A MATLAB® code was written to extract fermenters, FeRB, SRB,
195 methanogens, and methylators from the pyrosequencing data file using the assembled
196 databases.

197 Samples were oven-dried at 105 °C for 24 h, and then homogenized and ground
198 using an agate mortar and pestle before analysis for C/S content, elemental composition,
199 and total organic carbon. Each sample was analyzed three times with mean values
200 reported herein. Solid-phase C/S content of the sediment and biochar samples was
201 measured using a resistance furnace (Eltra CS-2000). The elemental compositions of the
202 sediment and biochars were obtained by digestion following EPA Method 3052 (multi-
203 acid digest with microwave assist) and analyzed by ICP-OES and ICP-MS. Total organic
204 carbon (TOC) analysis of the sediment followed these steps: 1) 0.5 g sediment was
205 digested with 40 mL of 10% H_2SO_4 for 30 min; 2) the extract was passed through a glass

fibre filter; 3) the filtrate was analyzed by a Skalar segmented flow analyzer using Standard Method 5310C to derive the value for TOC of the sediment.

2.5 Statistical Analysis

The correlation between the measured parameters was evaluated by calculation of Pearson product moment correlation coefficients (r). The significance of a correlation, r, was tested using a t test with a 95% confidence level ($P<0.05$). The similarity of each parameter between the duplicated sediment controls, OAK700-amended, and MANURE600-amended systems was tested by conducting a t-test with a 95% confidence level ($P<0.05$). A t-test was conducted to evaluate whether THg and MeHg concentrations in the amended systems were significantly different from sediment controls.

3 Results and Discussion

3.1 Overview of Sediment, River Water, and Biochar Samples

Microcosm experiments were conducted for 524 d under anaerobic conditions using sediment with a Hg concentration of 187 µg g^{-1}. Total elemental concentrations in the sediment were 300 µg g^{-1} S, 16 000 µg g^{-1} Fe, 150 µg g^{-1} Cu, and 230 µg g^{-1} Mn. The concentration of total organic carbon in the sediment was 17 600 µg g^{-1}. The river water contained <5 ng L^{-1} THg, <0.02 ng L^{-1} MeHg, and low concentrations of other elements.

The selection of these biochars was based on the pyrolysis temperature and their properties, including potential to release organic acids (OA), DOC, SO_4^{2-}, and heavy metals, content of C and S, and specific surface area. These parameters are known to influence Hg stabilization and MeHg production in natural systems, and biochars with a range of properties were selected to evaluate the influence of these properties during amendment. GRASS300 and GRASS600 were selected to compare the effect of pyrolysis

temperature on Hg stabilization and MeHg production. Low concentration of OA and DOC, and medium concentration of SO_4^{2-} are released by AC and GRASS600 (Table 1); low and medium concentrations of these components are released by OAK700 and GRASS300, respectively; low concentration of OA and DOC, and high concentration of SO_4^{2-} are released by MANURE600 (Liu et al., 2015; Liu et al., 2016). The reactive materials were rich in carbon (Table 1), e.g., 70.2% for GRASS300 and 94-99.9% for AC, OAK700, and GRASS600, with the exception of MANURE600 (18.5%). S content ranged from <0.1% for OAK700 to as high as 0.55% for GRASS600. The reactive materials except MANURE600 were low in other elements, including major and minor elements. The MANURE600 was rich in Al, Ca, Fe, K, Mg, Na, and P. The surface area of AC, OAK700, GRASS300, GRASS600 and MANURE600 was 600, 65, 2.6, 230, and 5.2 $m^2\ g^{-1}$.

3.2 Aqueous Chemistry

The pH of the sediment in the control and amended systems gradually increased from ~7.5 to ~9.0 over the first 150 d and then decreased slightly to ~8.5 by 445 d (Fig. 2). The pH values in the biochar controls increased rapidly from ~8.5 to ~9.2, then decreased gradually to ~8.5. The pH of the AC, GRASS600, and MANURE600 controls were greater than for other controls, which is consistent with previous observations from a batch study (Liu et al., 2015). Eh values for the controls and amended systems were similar and decreased from ~50 to ~-420 mV in the first 126 d, then decreased slightly to ~-440 mV until the experiments were terminated at 524 d. These Eh values indicate an anaerobic environment was maintained over the course of the experiment. No significant

252 differences were observed in the values of pH and Eh among sediment controls, biochar
253 controls, and amended systems (P<0.05).

254 **3.3 THg in Aqueous Phase**

255 The 0.2-µm filtered THg concentrations ranged from 0.8 to 32 µg L^{-1} for the sediment
256 controls and amended systems (Fig. 3). A gradual increase in concentrations of 0.2-µm
257 filtered THg was observed over the course of the experiment in the sediment controls and
258 MANURE600-amended systems; other amended systems showed a pattern featuring an
259 initial increase then slow decrease. The 0.2-µm THg concentrations for the amended
260 systems were less than for the sediment controls, except for the final samples collected in
261 the MANURE600-amended systems. THg concentrations in the duplicate systems
262 amended with OAK700 and MANURE600 were in good agreement. THg concentrations
263 for the AC- and GRASS300-amended systems were significantly lower than those for
264 sediment controls.

265 Concentrations of 0.45-µm filtered THg ranged from 1.0 to 50 µg L^{-1} for the
266 sediment controls and amended systems (Fig. 3). Compared with concentrations of 0.2-
267 µm THg, 0.45-µm THg concentrations were highly variable during the first 100 d, with a
268 spike in concentration observed at 30 d for the controls and amended systems. A gradual
269 increase in THg concentrations was observed in the sediment controls after the initial 23
270 d, then THg concentrations stabilized at ~30 and 50 µg L^{-1}. THg concentrations in
271 duplicate systems were not significantly different. THg concentrations for AC-,
272 GRASS300-, GRASS600-, and duplicated MANURE600-amended systems were
273 significantly lower than those for sediment controls after 100 days. The decrease of THg

274 from the microcosm experiment was not correlated with the specific surface area of the
275 biochars.

276 Ratios of 0.2- and 0.45-µm filtered THg concentrations were between 0.1 and 1.0
277 for sediment controls and AC, OAK700, GRASS300, and GRASS600 amended systems,
278 which was expected. However, ratios were between 1.2 and 3.9 for six sampling events
279 from MANURE600 amended systems, which indicates concentrations of 0.2-µm filtered
280 THg were higher than 0.45-µm filtered THg. The reason for ratios greater than 1.0 may
281 be due to the greater blockage of pore spaces in 0.45-µm filters than those in 0.2-µm
282 filters by organic matter or colloids in the aqueous phase.

283 The effectiveness of co-blending with respect to reducing aqueous 0.45-µm THg
284 concentrations was not obvious at early stages. THg concentrations decreased by 60 to 90%
285 (mean 75%) compared with the sediment control for the AC-amended system after 30 d,
286 by 20 to 60% (mean 46%) for the OAK700-amended system after 250 d, by 30 to 90%
287 (mean 69%) for the GRASS300-amended system after 100 d, by 20 to 70% (mean 39%)
288 for the GRASS600-amended system after 100 d, and by 40 to 92% (mean 70%) for the
289 MANURE600-amended systems after 30 d. An increase in THg concentrations was
290 observed in the MANURE600-amended systems after 126 d. THg concentrations were
291 <5 ng L^{-1} in the ultrapure water control and <50 ng L^{-1} in river water and biochar controls.

292 Concentrations of unfiltered THg in the sediment controls and amended systems
293 decreased from 400-700 µg L^{-1} at the beginning of the experiment to 20-80 µg L^{-1} at its
294 termination. Unfiltered concentrations were significantly greater than concentrations of
295 0.2- and 0.4-µm filtered THg (P<0.05). Spikes of unfiltered THg concentrations were
296 observed with values as high as 1670 µg L^{-1} at day 37 for a sediment control, 900 µg L^{-1}

297 at day 100 for the AC-amended system, and 1180 µg L^{-1} at day 37 for one
298 MANURE600-amended system. THg concentrations for the GRASS300-amended
299 system were all lower than those for the sediment controls and other amended systems.
300 No significant differences of unfiltered THg concentrations were observed among the
301 sediment controls and amended systems.

302 A previous batch experiment to evaluate Hg removal by the same biochars used in
303 this study showed removal rates greater than 90% from Hg-spiked river water (~10 µg L^{-1})
304 within 2 d (Liu et al., 2016). The reasons for the lower removals observed in this study
305 are likely multi-faceted but might include the fact that DOC can retain Hg in the aqueous
306 phase (Gomez-Eyles et al., 2013), blockage of adsorption sites by sediment particles
307 (Mayer, 1994), competing effects for adsorption sites from other cations (Herrero et al.,
308 2005), continuous release of Hg from the sediment (Pereira et al., 1998), and the
309 relatively high ratio of total Hg to biochar (18.7 mg THg to 5 g biochar).

310 In the GRASS300-amended system, the concentrations of 0.2-µm, 0.45-µm, and
311 unfiltered THg were less than the corresponding concentrations of sediment controls and
312 other amended systems. These results indicate GRASS300 is the most promising reactive
313 material to stabilize Hg in contaminated sediment under anaerobic conditions. This
314 observation is different from the previous batch-style experiment with respect to the
315 addition of biochar to Hg-spiked river water (Liu et al., 2016), which showed the least
316 amount of THg removed by GRASS300 compared with AC, OAK700, GRASS600, and
317 MANURE600.

3.4 MeHg in aqueous phase

Two peak MeHg concentrations were observed in the sediment controls and amended systems (Fig. 3). Early peaks in concentrations were observed at day 37 (48 ng L^{-1}) and day 47 (130 ng L^{-1}) in the duplicate sediment controls. MeHg concentration peaks in the amended systems were lower than those in sediment controls for most concurrent data points, with the exception that the peak in the AC-amended system was greater than one of the sediment controls. The concentrations at this first peak were <13 ng L^{-1} for the OAK700-, GRASS300-, and GRASS600-amended systems, and 38 ng L^{-1} for the MANURE600-amended system. A second peak was observed in the duplicate sediment controls with concentrations as high as 64 and 28 ng L^{-1}. The second peaks in the AC-, GRASS300-, and MANURE600-amended systems were much lower than those in the sediment controls, while the second peaks in the OAK700- and GRASS600-amended systems were much greater with MeHg concentrations of 220 and 260 ng L^{-1}, respectively. However, due to sampling events, the water level decreased over time in the systems, and the calculated mass of MeHg at the second peak in the OAK700- and GRASS600-amended systems was less than that at the first peak of the sediment controls (Fig. 3). MeHg concentrations of river water and biochar controls were below the MDL.

MeHg concentrations in AC-, GRASS300-, and GRASS600-amended systems were significantly lower than those in sediment controls for the first 200 d. Ratios of MeHg to 0.45 µm-filtered THg concentrations ranged from 0.01 to 2.6% (most < 0.1%) for sediment controls and amended systems, and no significant correlation were observed between MeHg and THg concentrations (Fig. S1; $P<0.05$). Ratios in estuarine waters (Al‐Madfa et al., 1994; Kannan et al., 1998) and freshwaters (Gill and Bruland, 1990;

Lee and Hultberg, 1990) range from 5 to 80%, which is much higher than those measured in the current study. The lower ratios in the present study were likely due to the elevated THg concentrations in the solutions.

A number of parameters affect the rates of MeHg production, including the availability of substrates for Hg methylators and competing organisms, temperature, pH, organic material, redox conditions, and bioavailable Hg species (Ullrich et al., 2001). Correlation analyses were performed between MeHg concentrations and other parameters measured during the experiment, including pH, Eh, alkalinity, THg, cations, anions, DOC, UV_{254}, $SUVA_{254}$, and nutrients. Aqueous MeHg concentrations were negatively correlated with SO_4^{2-} concentrations in all systems. MeHg concentrations were consistently positively correlated with unfiltered THg (Fig. 3) in sediment controls. For most amended systems, MeHg concentrations were positively correlated with concentrations of unfiltered THg, alkalinity, DOC, Mn, and Fe. Alkalinity and DOC are carbon energy sources for microbes, including Hg methylators. Fe, Mn, and SO_4^{2-} are electron acceptors for FeRB and SRB, which are potential Hg methylators (Benoit et al., 2001; Gilmour et al., 1992; Kerin et al., 2006; Yu et al., 2011). Additionally, aqueous MeHg concentrations can also be influenced by partitioning to the solid phase, demethylation reactions, and other parameters (Benoit et al., 2003; Ortiz et al., 2015).

3.5 MeHg in solid phase

The solid-phase MeHg content ranged from 8 to 35 ng g^{-1} in the sediment controls and AC-amended systems, one of the OAK700 duplicates, and a MANURE600 duplicate (Fig. 4). The MeHg contents in the amended systems were not significantly different from sediment controls, and contents in the OAK700-, GRASS300-, and GRASS600-

amended systems were even greater than the sediment controls at later sampling events. A sharp increase of MeHg content was observed for the last two sampling events in an OAK700 duplicate, the GRASS300-amended system, and the GRASS600-amended system to values of up to 260 ng g^{-1}. The elevated MeHg content of the OAK700- and GRASS600-amended systems corresponds to the elevated aqueous MeHg concentrations (Fig. 3).

These results indicate the application of AC and biochar does not result in an obvious decrease in MeHg content in the solid phase, unlike the aqueous MeHg concentration. This observation is consistent with previous studies (Huntington et al., 2015; Lewis et al., 2016), that suggest the application of AC results in the sorption of MeHg to AC thereby decreasing aqueous MeHg concentrations. Shu et al. (2016) and Zhang et al. (2018) also report an increase of MeHg content in paddy soils after the addition of biochars. Gomez-Eyles et al. (2013) observed a decrease in aqueous MeHg concentrations in AC and biochar amended systems and attributed this decrease to sorption rather than inhibition of MeHg production. However, Bussan et al. (2016) report a decrease in MeHg content in sediment after the addition of biochar or AC, and attribute this decrease to a decrease in Hg bioavailability after the addition of biochar or AC. This inconsistency is likely due to differences in experimental conditions, including soil or sediment type, biochar composition and other parameters such as pH, Eh, organic matter content and availabilities of electron acceptors such as Fe^{3+} and SO_4^{2-}.

Distribution coefficients (K_d) were calculated using measured concentrations of MeHg in the solid and aqueous phases at different times during the experiment (Fig. 5). K_d values ranged from 200 to 18000 L kg^{-1} and no clear patterns were observed versus

time. This result indicates that K_d is not likely a proper parameter to describe the distribution of MeHg between the solid and aqueous phases in this study, which is inconsistent with a previous study (Gomez-Eyles et al., 2013). Therefore, the distribution of MeHg between the solid and aqueous phases in the present study was likely controlled by other processes.

3.6 Carbon Sources for Microbes

Acetate, formate, propionate, DOC, and alkalinity are potential carbon sources for microorganisms. Concentrations of acetate, formate, propionate, and alkalinity increased and then decreased in sediment controls and amended systems over the course of the experiment (Fig. 6). The DOC concentrations in most systems continued to increase, with the exception of a spike in the AC-amended system.

A peak in acetate concentration was observed in each system, with concentrations of up to 41 mg L^{-1} for sediment controls and ranging from 21 mg L^{-1} for the OAK700-amended system to 226 mg L^{-1} for the AC-amended system. The peak occurred at day 168 for the sediment controls and ranged from day 112 to 387 for the amended systems. No great difference in acetate concentrations was evident between the sediment controls and amended systems, with the exception of the spike in the AC-amended system. Acetate concentrations were <1 mg L^{-1} for most biochar control data points; the exception was the spike in concentrations for AC- and GRASS300-amended systems (5.0-89 mg L^{-1}). Elevated formate and propionate concentrations were also observed in the sediment controls and amended systems. Similar trends were observed for concentrations of acetate, formate, and propionate, except peak concentrations of formate and propionate were much lower than those of acetate.

410 DOC concentrations increased from 2 to 80 mg L^{-1} for the sediment controls and
411 amended systems, except for a spike (340 mg L^{-1}) in the AC-amended system that
412 corresponded to peak acetate and alkalinity concentrations. The increasing trend with
413 time was observed in both the sediment controls and amended systems, while the
414 concentrations of DOC in the AC- and MANURE600-amended systems were lower than
415 those of sediment controls. The DOC concentrations in biochar controls were less than 2
416 mg L^{-1} before day 154 and increased to as high as 400 mg L^{-1}.

417 Concentrations of organic acids and DOC in the microcosm experiments were
418 much greater than in a previous batch experiment using the same biochars (Table 1; Liu
419 et al. (2015)). The results indicate the organic acids and DOC released by biochars have
420 limited contributions to concentrations in the microcosm experiment. The increase in
421 organic acids and DOC concentrations in the microcosm experiments is likely related to
422 the organic matter in the sediment (17 600 µg g^{-1}).

423 Alkalinity increased from ~50 to ~200 mg L^{-1} before day 100 and then decreased
424 to ~50 mg L^{-1} at day 445 in both the sediment controls and amended systems. The
425 alkalinity concentrations of biochar controls varied slightly between 50 and 100 mg L^{-1}.
426 The increase in alkalinity in sediment controls and amended systems is likely a result of
427 microbial activity by utilizing the organic matter (17 600 µg g^{-1}) from the sediment. The
428 decrease in alkalinity is likely due to consumption by methanogens or the formation of
429 carbonate minerals.

430 The absorption of UV_{254} is generally greatest for aromatic molecules (Silverstein
431 et al., 1974; Weishaar et al., 2003). $SUVA_{254}$ is defined as the UV_{254} measured in m^{-1}
432 divided by the concentration of DOC in mg L^{-1} (Weishaar et al., 2003) and is a surrogate

433 measure for the aromaticity of DOC. The absorbance of UV_{254} increased from 0 to ~2.8
434 cm^{-1} in the sediment controls and OAK700-, GRASS300-, GRASS600-, and
435 MANURE600-amended systems, and the increasing trend in absorbance was consistent
436 with the increasing trend of DOC concentrations (Fig. 6). The absorbance in the AC-
437 amended system (up to 0.5 cm^{-1}) was significantly lower than for the sediment controls
438 and other amended systems. $SUVA_{254}$ values varied by only ~3 L mg^{-1} m^{-1} in the
439 sediment controls and OAK700-, GRASS300-, GRASS600-, and MANURE600-
440 amended systems over the course of the experiment; these consistent $SUVA_{254}$ values
441 indicate the aromaticity of the DOM did not greatly change over the course of the
442 experiment. $SUVA_{254}$ values in the AC-amended system decreased from 4.5 to as low as
443 0.1 L mg^{-1} m^{-1}. The results indicate the aromaticity of the DOM in the AC-amended
444 system was significantly lower than in the sediment controls and other amended systems.
445 No significant correlations were observed between $SUVA_{254}$ and Hg species, including
446 0.2- and 0.45-µm filtered THg and 0.45-µm filtered MeHg.

447 DOC plays an important role in Hg speciation in the aqueous phase. Lower DOC
448 concentrations were observed in the AC- and MANURE600-amended systems than in the
449 sediment controls, which corresponded to lower aqueous THg concentrations in the AC-
450 and MANURE600-amended systems compared with sediment controls at early stages
451 (Fig. 3). For the OAK700-, GRASS300-, and GRASS600-amended systems, DOC
452 concentrations were similar or higher than those in the sediment controls at early stages
453 and THg concentrations were less than the sediment controls after extended periods.
454 These observations are consistent with previous studies (Gilmour et al., 2013; Gomez-
455 Eyles et al., 2013) in which aqueous inorganic Hg was controlled in sediments and

456 reactive media (AC and biochar) co-blending experiments when DOC concentrations
457 remained low. Hg-DOC complexes readily form in solution. These complexes are stable
458 and can maintain elevated concentrations of Hg in the aqueous phase (Gomez-Eyles et al.,
459 2013). The presence of DOC can also prevent the precipitation of HgS nanoparticles
460 (Aiken et al., 2011). DOC can also be utilized as a carbon source by potential Hg
461 methylators and can enhance the bioavailability of Hg by facilitating Hg uptake for
462 potential methylators (Chiasson-Gould et al., 2014).

463 **3.7 Electron Acceptors for Microbes**

464 Concentrations of NO_3^-, Mn, Fe, and SO_4^{2-} are plotted in Fig. 7 in decreasing order of
465 energetically favourable electron-accepting reactions for microbial respiration. NO_3^-
466 concentrations decreased from ~45 mg L^{-1} to <MDL (0.05 mg L^{-1}) within 9 d for the
467 sediment controls and amended systems. Dissolved Mn concentrations increased from
468 <0.005 to ~1.2 mg L^{-1} within 65 d and decreased to <0.2 mg L^{-1} after 154 d in the
469 sediment controls and amended systems. A lag stage of dissolved Fe concentrations (<0.2
470 mg L^{-1}) was observed for the first 23 d in the sediment controls and amended systems; Fe
471 concentrations then increased to peak concentrations ranging from 0.47 to 3.5 mg L^{-1} at
472 day 100 and then decreased to <0.2 mg L^{-1} after 154 d. Dissolved Fe concentrations in the
473 AC-amended system were lower than in the sediment controls and other amended
474 systems. SO_4^{2-} concentrations increased slightly at the first 37 d and then decreased to
475 <MDL (0.05 mg L^{-1}) after 79 d for the sediment controls, 65 d for the GRASS300-
476 amended system, 89 d for the OAK700-amended system, 100 d for the AC- and
477 GRASS600-amended systems, and 126 d for the MANURE600-amended system. Due to

478 the rapid shift to anaerobic conditions (Fig. 2), the reduction of Fe and SO_4^{2-} occurred
479 simultaneously.

480 Concentrations of NO_3^-, Mn, and Fe in the aqueous solution of the amended
481 systems were derived from the sediment, because they were elevated in the sediment
482 solids and generally less than the analytical detection limits in the aqueous phase of
483 biochar controls (Fig. 7), the river water, and the solid phase biochars (Table 1). For
484 biochar and river water controls, NO_3^- concentrations decreased from ~2 mg L^{-1} to
485 <MDL; Mn concentrations were <0.05 mg L^{-1}, except one data point from the
486 GRASS300 control; and Fe concentrations were <0.02 mg L^{-1}. A fraction of the SO_4^{2-} in
487 the aqueous solution of the amended systems was released from the biochars. The initial
488 SO_4^{2-} concentrations of the biochar controls, which occur in the order MANURE600 >
489 AC > GRASS600 > GRASS300 > OAK700, is consistent with a previous batch-style
490 experiment (Liu et al., 2016). The SO_4^{2-} concentrations of biochar controls decreased
491 slightly over 445 d, which indicates suitable substrates for the growth of SRB were not
492 likely provided by the biochar. The elevated SO_4^{2-} concentration in the MANURE600-
493 amended system is likely due to the elevated S content and inorganic sulfate fraction in
494 this system (Liu et al., 2016). The concentrations of NO_3^-, Mn, Fe, and SO_4^{2-} in aqueous
495 phase were affected by their contents in sediment and biochar and also the partitioning
496 among phases.

497 Concentrations of SO_4^{2-} in the GRASS300-amended system decreased fastest
498 among all the amended systems. This decrease may be a result of the greater fraction of
499 labile organic carbon in GRASS300. Previous studies have shown that low-temperature
500 biochars have organic carbon that is more labile compared to high-temperature biochar

501 (Bruun et al., 2011; Cross and Sohi, 2011). These elevated concentrations of labile
502 organic carbon can promote SRB activity. The rapid decrease in SO_4^{2-} for GRASS300 is
503 associate with an early decrease in THg. This removal could be due to the formation of
504 Hg-S minerals, causing a decrease in Hg bioavailability, possibly explaining the lower
505 aqueous MeHg concentrations observed in the GRASS300-amended system.
506 The increase in 0.45-μm filtered THg concentrations after 23 d corresponds to the
507 increase in dissolved total Fe concentrations, which indicates Fe(II) is likely released due
508 to the reduction of Fe(III) minerals together with adsorbed Hg. The decrease in 0.45-μm
509 filtered THg in the amended systems was likely due to the formation of Hg-sulfide
510 precipitates as a result of SO_4^{2-} reduction. The maximum decreases in Fe and SO_4^{2-}
511 concentrations corresponded to the first peak in MeHg in the sediment controls and
512 amended systems; Fe concentrations were positively correlated with MeHg
513 concentrations (P<0.05) in the AC- and MANURE600-amended systems.
514 Previous batch experiments indicate elevated concentrations of organic acids,
515 DOC (Liu et al., 2015), and SO_4^{2-} (Liu et al., 2016) are released by AC, GRASS300, and
516 MANURE600, suggesting the addition of biochars might stimulate MeHg production.
517 However, the microcosm experiments indicate that MeHg concentrations minimally
518 increased in the presence of these biochars at early stages.
519 **3.8 Nutrients in the aqueous phase**
520 Nutrients are essential for the growth and activity of microbes. Similar trends were
521 observed for NH_3-N and PO_4-P in sediment controls and amended systems (Fig. 8). The
522 concentrations of NH_3-N and PO_4-P in sediment controls increased from <MDL to ~6
523 and 4.5 mg L^{-1}, respectively. Concentrations of NH_3-N and PO_4-P were lower in AC-,

524 OAK700-, GRASS300-, and GRASS600-amended systems than in sediment controls.
525 NH_3-N and PO_4-P concentrations in MANURE600-amended systems were higher than in
526 sediment controls, likely due to the elevated nutrient content in the manure (Table 1).
527 Nutrient concentrations were typically lower in biochar controls than sediment controls
528 and amended systems, which indicates the nutrients originated from the sediment.
529 Concentrations of NH_3-N and PO_4-P were positively correlated with DOC concentrations
530 in sediment controls and each amended system. This observation indicates the increase of
531 nutrient concentrations is likely due to the degradation of N- and P-containing organic
532 matter in the sediment. Nutrient concentrations were typically lower in biochar controls
533 than sediment controls and amended systems, which indicates the nutrients originated
534 from the sediment.

535 **3.9 Pyrosequencing**

536 The percentages of fermenters, FeRB, SRB, and methanogens at the genus level were
537 extracted from the pyrosequencing data and plotted in Fig. 9. The sum of the percentages
538 for all categories increased with time. Similar increasing and then decreasing patterns
539 were observed over time for fermenters, FeRB, and SRB, but abundances ranged from
540 4.9 to 25%, 4.8 to 20%, and 0.8 to 3.5%, respectively. Fermenters were present in
541 moderate numbers over the course of the experiment. SRB were consistently in low
542 abundance during the experiment, likely due to the low initial concentration of sulfate.
543 The percentage of methanogens consistently increased over time from 0% to as high as
544 70%. Percentages of extracted 16s rRNA in the duplicated OAK700- and MANURE600-
545 amended systems were in good agreement. The similar patterns between sediment
546 controls and amended systems suggest the addition of biochars had little impact on the

547 microbial community. This observation is consistent with previous studies (Kelly et al.,
548 2014; Noyce et al., 2015) in which the microbial communities were not affected after the
549 addition of biochar.

550 Under sufficiently reducing conditions, fermenters and other microorganisms can
551 degrade organic matter (OM) in sediment to form DOC and short-chain OA, as indicated
552 by Equ. 1. Oxidation of organic carbon (17 600 μg g^{-1}) in the South River sediment might
553 explain the changes in DOC and short-chain organic acid concentrations in solution (Fig.
554 6). The labile organic carbon forms within DOC are key carbon and energy sources for
555 nitrate-reducing bacteria (Hagman et al., 2008), FeRB (Lovley, 1991), SRB (Muyzer and
556 Stams, 2008), and methanogens (Deppenmeier, 2002), and many of FeRB, SRB, and
557 methanogens are potential Hg methylators. The increase in alkalinity during early stages
558 of the experiments might be due to the respiration of fermenters, nitrate-reducing bacteria,
559 FeRB, and SRB (Equs. 1-4). Nitrate-reducing bacteria can reduce nitrate to other forms
560 of N (complete process indicated by Equ. 2). Because NO_3^- concentrations were <MDL
561 at 7 d and the first sample for pyrosequencing analysis was collected at 65 d, nitrate-
562 reducing bacteria were not extracted from the pyrosequencing results. The FeRB can
563 reduce oxidized solid-phase forms of Mn and Fe and release reduced aqueous forms (Fig.
564 7; Equ. 3) (Ribet et al. (1995)). The SRB can reduce SO_4^{2-} to S^{2-} (Equ. 4) (Moncur et al.
565 (2015) Lindsay et al. (2011)); the production of S^{2-} can then be consumed by the
566 formation of Fe- (Equ. 5) (Benner et al. (2002) and Hg-sulfide minerals (Equ. 6). The
567 formation of these minerals explains the decrease in dissolved Hg and Fe over time (Figs.
568 3, 7). Methanogens can utilize carbon sources, including inorganic carbon, formate, and

acetate (Deppenmeier, 2002), as energy sources (Equ. 7), and the increase in methanogen abundance corresponds to the decrease in alkalinity (Fig. 6).

$$OM_{(s)} \rightarrow DOC + OA + HCO_3^- \quad \text{Equ. 1}$$

$$4NO_3^- + 5CH_2O = 2N_2 + 5HCO_3^- + 2H_2O + H^+ \quad \text{Equ. 2}$$

$$4Fe(OOH) + CH_2O + 7H^+ = 4Fe^{2+} + HCO_3^- + 6H_2O \quad \text{Equ. 3}$$

$$SO_4^{2-} + 2CH_2O = HS^- + 2HCO_3^- + H^+ \quad \text{Equ. 4}$$

$$Fe^{2+} + HS^- = FeS_{(s)} + H^+ \quad \text{Equ. 5}$$

$$Hg^{2+} + HS^- = HgS_{(s)} + H^+ \quad \text{Equ. 6}$$

$$CO_2 + 4H_2 = CH_4 + 2H_2O \quad \text{Equ. 7}$$

Twelve potential methylators at the species level were obtained from the pyrosequencing results, including fermenters, FeRB, SRB, and methanogens (Fig. 10). Their total abundance was <0.7%. A general increasing and decreasing pattern of the total abundance of potential methylators is evident (Fig. 10). The abundance of the potential methylators is not well correlated with concentrations of MeHg in the aqueous and solid phases, which indicates that quantification of known potential methylator abundances might not be a good indicator for net MeHg concentration in aqueous and solid phases. The late MeHg spikes in the OAK700- and GRASS600-amended systems do not correspond with a spike in the known potential methylators at day 387, which suggests unknown methylators likely existed in these two systems. This discrepancy might also be a result of the limitation of the database used for pyrosequencing data analysis. A large fraction of the microorganisms in the environment is not represented in the database (Rondon et al., 1999).

Column experiments conducted by Desrochers et al. (2015) and Paulson et al. (2016) show that MeHg production in the South River sediment could be stimulated by increasing the concentrations of electron donors and acceptors at a proper ratio. Here, less

MeHg was observed in the aqueous phase in the amended systems using AC, GRASS300, and MANURE600 than for sediment controls even with slightly elevated carbon sources, electron acceptor (SO_4^{2-}), and percentages of methylators in the amended systems.

The following processes are proposed to describe the decrease of Hg and MeHg in the aqueous phase after addition of the amendments. First, a rapid release of dissolved Hg from the sediment and rapid adsorption by biochars occurs. Hg concentrations do not decrease due to continuous dissolution of soluble Hg phases and because binding between Hg and biochar is generally weak; rapid nitrate reduction also happens in this stage. The second stage is a Fe-reducing period. Hg retained in Fe-oxide minerals is released into solution after reductive dissolution of Fe-oxide minerals. Hg is weakly adsorbed by biochars and MeHg is produced by FeRB (Kerin et al., 2006; Yu et al., 2011). The third stage is a sulfate reducing period. Sulfate is reduced to sulfide, and Hg binds with sulfide and forms Hg-S precipitates on the surface or inside the pores of biochar particles (Liu et al., 2017). The formerly adsorbed Hg might also be converted to Hg-S minerals (Liu et al., 2017). The binding between Hg and the biochar particles is strong, and less MeHg is produced by SRB (Benoit et al., 2001; Gilmour et al., 1992) due to the low bioavailability of Hg after stabilization by the biochars. The fourth stage is a methanogenic period. MeHg is produced by methanogens (Hamelin et al., 2011; Yu et al., 2013). The early MeHg concentration peaks in the aqueous phase are attributed to the activity of fermenters, FeRB, and SRB and the late peaks are attributed to the activity of methanogens. Methanogens capable of methylation likely existed in the OAK700- and GRASS600-amended systems.

4 Conclusion

These microcosm experiments indicate that biochar-amended systems can be effective in reducing Hg concentrations in the aqueous phase. The presence of biochar appears to have a limited impact on microbial community structure. The removal of Hg using biochars is comparable to that achieved by the application of AC. A late MeHg concentration spike occurred in the OAK700- and GRASS600-amended systems. But, for the majority of the biochar types evaluated, Hg and MeHg concentrations in the aqueous phase (and potentially the bioavailability) tend to decrease after biochar amendment. The stabilization of Hg is attributed to the formation of Hg-sulfide minerals and precipitation on or within biochar particles.

The results indicate GRASS300 is the most promising reactive material for Hg stabilization of contaminated sediment. If GRASS300 is applied in the field, special attention should be paid to its physical breakdown (Spokas et al., 2014). During the experiment, GRASS300 was observed to be more fragile than wood-derived biochars. For the application of most types of biochar in water bodies, another challenge is how to maintain the biochar in the desired locations due to its low density and settling rate (Gomez-Eyles et al., 2013). During sampling events, many biochar particles were observed at the interface between the aqueous and solid phase and biochar particles could be easily relocated by the movement of the water. This problem could be addressed by encasing the biochar particles using geotextile (Shackley et al., 2016) before field applications.

This study indicates that the physical and chemical properties affect the potential for biochar to control Hg concentrations and induce methylation when used as a sediment amendment. Other properties that may also influence the effectiveness of biochar as an

amendment include the volatile (labile) versus fixed carbon content, ash content, mineral content, calcium carbon equivalent, pore size distribution, and S speciation and distribution. Measurement of these parameters could assist in further interpretation of the results.

At the termination of the experiment, biochar particles were easily distinguished from the sediment, which indicates the biochar remained stable over the course of the experiment. This observation is consistent with previous studies that indicate biochar can be stable in the environment (Mann, 2002; Spokas, 2010). The Hg that accumulated in the biochar through this process is expected to remain stable for a prolonged period. Further, this process can also be extended to the accumulation of other hazardous metal elements.

Acknowledgments

Funding for this research was provided by the Natural Sciences and Engineering Research Council of Canada, E. I. du Pont de Nemours and Company, and the Canada Research Chairs program. We thank J. Ma, Y. Liu, A.O. Wang, and K. Paulson for assistance with chemical analyses. We also thank L. Hug from the University of Waterloo; D. Peak from the University of Saskatchewan; R. C. Landis, J. Dyer, E. Mack, and N. Grosso from E. I. du Pont de Nemours and Company; S. Brooks from Oak Ridge National Laboratory; and members of the South River Science Team for their advice on the results of the study.

References

Ahmad, M., Rajapaksha, A.U., Lim, J.E., Zhang, M., Bolan, N., Mohan, D., Vithanage, M., Lee, S.S., Ok, Y.S., 2014. Biochar as a sorbent for contaminant management in soil and water: a review. Chemosphere 99, 19-23. Doi: 10.1016/j.chemosphere.2013.10.071.

Aiken, G.R., Hsu-Kim, H., Ryan, J.N., 2011. Influence of dissolved organic matter on the environmental fate of metals, nanoparticles, and colloids. Environ. Sci. Technol. 45, 3196-3201. Doi: 10.1021/es103992s.

Al‐Madfa, H., Dahab, O.A., Holail, H., 1994. Mercury pollution in Doha (Qatar) coastal environment. Environ. Toxicol. Chem. 13, 725-735. Doi: 10.1002/etc.5620130506.

Benner, S.G., Blowes, D.W., Ptacek, C.J., Mayer, K.U., 2002. Rates of sulfate reduction and metal sulfide precipitation in a permeable reactive barrier. Appl. Geochem. 17, 301-320. Doi: 10.1016/S0883-2927(01)00084-1.

Benoit, J., Gilmour, C., Heyes, A., Mason, R., Miller, C., 2003. Geochemical and biological controls over methylmercury production and degradation in aquatic ecosystems, ACS Symp. Ser., pp. 262-297.

Benoit, J.M., Gilmour, C.C., Mason, R.P., 2001. Aspects of bioavailability of mercury for methylation in pure cultures of *Desulfobulbus propionicus* (1pr3). Appl. Environ. Microbiol. 67, 51-58. Doi: 10.1128/AEM.67.1.51-58.2001.

Bruun, E.W., Hauggaard-Nielsen, H., Ibrahim, N., Egsgaard, H., Ambus, P., Jensen, P.A., Dam-Johansen, K., 2011. Influence of fast pyrolysis temperature on biochar labile fraction and short-term carbon loss in a loamy soil. Biomass Bioenerg. 35, 1182-1189. Doi: 10.1016/j.biombioe.2010.12.008.

Bundschuh, M., Zubrod, J.P., Seitz, F., Newman, M.C., 2015. Effects of two sorbents applied to mercury-contaminated river sediments on bioaccumulation in and detrital processing by *Hyalella azteca*. J. Soils Sediments 15, 1265-1274. Doi: 10.1007/s11368-015-1100-z.

Bussan, D.D., Sessums, R.F., Cizdziel, J.V., 2016. Activated carbon and biochar reduce mercury methylation potentials in aquatic sediments. Bull. Environ. Contam. Toxicol. 96, 536-539. Doi: 10.1007/s00128-016-1734-6.

Cheng, H., Hu, Y., 2012. Mercury in municipal solid waste in China and its control: a review. Environ. Sci. Technol. 46, 593-605. Doi: 10.1021/es2026517.

Chiasson-Gould, S.A., Blais, J.M., Poulain, A.J., 2014. Dissolved organic matter kinetically controls mercury bioavailability to bacteria. Environ. Sci. Technol. 48, 3153-3161. Doi: 10.1021/es4038484.

Clarkson, T.W., Magos, L., 2006. The toxicology of mercury and its chemical compounds. Crit. Rev. Toxicol. 36, 609-662. Doi: 10.1080/10408440600845619.

Cross, A., Sohi, S.P., 2011. The priming potential of biochar products in relation to labile carbon contents and soil organic matter status. Soil Biol. Biochem. 43, 2127-2134. Doi: 10.1016/j.soilbio.2011.06.016.

Deppenmeier, U., 2002. The unique biochemistry of methanogenesis. Prog. Nucleic. Acid Res. Mol. Biol. 71, 223-283. Doi: 10.1016/S0079-6603(02)71045-3.

Desrochers, K.A.N., Paulson, K.M.A., Ptacek, C.J., Blowes, D.W., Gould, W.D., 2015. Effect of electron donor to sulfate ratio on mercury methylation in floodplain

sediments under saturated flow conditions. Geomicrobiol. J. 32, 924-933. Doi: 10.1080/01490451.2015.1035818.

Gibson, B.D., Ptacek, C.J., Lindsay, M.B.J., Blowes, D.W., 2011. Examining mechanisms of groundwater Hg(II) treatment by reactive materials: an EXAFS study. Environ. Sci. Technol. 45, 10415-10421. Doi: 10.1021/es202253h.

Gill, G.A., Bruland, K.W., 1990. Mercury speciation in surface freshwater systems in California and other areas. Environ. Sci. Technol. 24, 1392-1400. Doi: 10.1021/es00079a014.

Gilmour, C.C., Henry, E.A., Mitchell, R., 1992. Sulfate stimulation of mercury methylation in freshwater sediments. Environ. Sci. Technol. 26, 2281-2287. Doi: 10.1021/es00035a029.

Gilmour, C.C., Riedel, G.S., Riedel, G., Kwon, S., Landis, R., Brown, S.S., Menzie, C.A., Ghosh, U., 2013. Activated carbon mitigates mercury and methylmercury bioavailability in contaminated sediments. Environ. Sci. Technol. 47, 13001-13010. Doi: 10.1021/es4021074.

Gomez-Eyles, J.L., Yupanqui, C., Beckingham, B., Riedel, G., Gilmour, C., Ghosh, U., 2013. Evaluation of biochars and activated carbons for *in situ* remediation of sediments impacted with organics, mercury, and methylmercury. Environ. Sci. Technol. 47, 13721-13729. Doi: 10.1021/es403712q.

Hagman, M., Nielsen, J.L., Nielsen, P.H., Jansen, J.l.C., 2008. Mixed carbon sources for nitrate reduction in activated sludge-identification of bacteria and process activity studies. Water Res. 42, 1539-1546. Doi: 10.1016/j.watres.2007.10.034.

Hamelin, S., Amyot, M., Barkay, T., Wang, Y., Planas, D., 2011. Methanogens: principal methylators of mercury in lake periphyton. Environ. Sci. Technol. 45, 7693-7700. Doi: 10.1021/es2010072.

Han, F.X., Su, Y., Monts, D.L., Waggoner, C.A., Plodinec, M.J., 2006. Binding, distribution, and plant uptake of mercury in a soil from Oak Ridge, Tennessee, USA. Sci. Total Environ. 368, 753-768. Doi: 10.1016/j.scitotenv.2006.02.026.

Herrero, R., Lodeiro, P., Rey-Castro, C., Vilariño, T., Sastre de Vicente, M.E., 2005. Removal of inorganic mercury from aqueous solutions by biomass of the marine macroalga *Cystoseira baccata*. Water Res. 39, 3199-3210. Doi: 10.1016/j.watres.2005.05.041.

Hilber, I., Bucheli, T.D., 2010. Activated carbon amendment to remediate contaminated sediments and soils: A review. Global Nest J. 12, 305-317.

Horvat, M., Bloom, N.S., Liang, L., 1993. Comparison of distillation with other current isolation methods for the determination of methyl mercury compounds in low-level environmental samples Part 1. Sediments. Anal. Chim. Acta 281, 135-152. Doi: 10.1016/0003-2670(93)85348-N.

Huntington, T.G., Lewis, A., Amirbahman, A., Marvin-DiPasquale, M.C., Culbertson, C.W., 2015. Assessment of the use of sorbent amendments for reduction of mercury methylation in wetland sediments at Acadia National Park, Maine: U.S. Geological Survey Scientific Investigations Report 2014-5234. US Geological Survey.

Jackson, T.A., 2016. Historical variations in the stable isotope composition of mercury in a sediment core from a riverine lake: effects of dams, pulp and paper mill wastes,

751 and mercury from a chlor-alkali plant. Appl. Geochem. 71, 86-98. Doi:
752 10.1016/j.apgeochem.2016.06.001.
753 Kannan, K., Smith Jr, R.G., Lee, R.F., Windom, H.L., Heitmuller, P.T., Macauley, J.M.,
754 Summers, J.K., 1998. Distribution of total mercury and methyl mercury in water,
755 sediment, and fish from South Florida estuaries. Arch. Environ. Contam. Toxicol.
756 34, 109-118. Doi: 10.1007/s002449900294.
757 Kelly, C.N., Peltz, C.D., Stanton, M., Rutherford, D.W., Rostad, C.E., 2014. Biochar
758 application to hardrock mine tailings: Soil quality, microbial activity, and toxic
759 element sorption. Appl. Geochem. 43, 35-48. Doi:
760 10.1016/j.apgeochem.2014.02.003.
761 Kerin, E.J., Gilmour, C.C., Roden, E., Suzuki, M.T., Coates, J.D., Mason, R.P., 2006.
762 Mercury methylation by dissimilatory iron-reducing bacteria. Appl. Environ.
763 Microbiol. 72, 7919-7921. Doi: 10.1128/aem.01602-06.
764 Lee, Y.-H., Hultberg, H., 1990. Methylmercury in some Swedish surface waters. Environ.
765 Toxicol. Chem. 9, 833-841. Doi: 10.1002/etc.5620090703.
766 Lewis, A.S., Huntington, T.G., Marvin-Dipasquale, M.C., Amirbahman, A., 2016.
767 Mercury remediation in wetland sediment using zero-valent iron and granular
768 activated carbon. Environ. Pollut. 212, 366-373. Doi:
769 10.1016/j.envpol.2015.11.047.
770 Li, H., Dong, X., da Silva, E.B., de Oliveira, L.M., Chen, Y., Ma, L.Q., 2017.
771 Mechanisms of metal sorption by biochars: biochar characteristics and
772 modifications. Chemosphere 178, 466-478. Doi:
773 10.1016/j.chemosphere.2017.03.072.
774 Light, T.S., 1972. Standard solution for redox potential measurements. Anal. Chem. 44,
775 1038-1039. Doi: 10.1021/ac60314a021.
776 Lindsay, M.B., Blowes, D.W., Ptacek, C.J., Condon, P.D., 2011. Transport and
777 attenuation of metal(loid)s in mine tailings amended with organic carbon: Column
778 experiments. J. Contam. Hydrol. 125, 26-38. Doi: 10.1016/j.jconhyd.2011.04.004.
779 Liu, P., Ptacek, C.J., Blowes, D.W., Berti, W.R., Landis, R.C., 2015. Aqueous leaching
780 of organic acids and dissolved organic carbon from various biochars prepared at
781 different temperatures. J. Environ. Qual. 44, 684-695. Doi:
782 10.2134/jeq2014.08.0341.
783 Liu, P., Ptacek, C.J., Blowes, D.W., Landis, R.C., 2016. Mechanisms of mercury removal
784 by biochars produced from different feedstocks determined using X-ray
785 absorption spectroscopy. J. Hazard. Mater. 308, 233-242. Doi:
786 10.1016/j.jhazmat.2016.01.007.
787 Liu, P., Ptacek, C.J., Blowes, D.W., Finfrock, Y.Z., Gordon, R.A., 2017. Stabilization of
788 mercury in sediment by using biochars under reducing conditions. J. Hazard.
789 Mater. 325, 120-128. Doi: 10.1016/j.jhazmat.2016.11.033.
790 Lovley, D.R., 1991. Dissimilatory Fe(III) and Mn(IV) reduction. Microbiol. Rev. 55,
791 259-287. Doi: 10.1016/S0065-2911(04)49005-5.
792 Mann, C.C., 2002. The real dirt on rainforest fertility. Science 297, 920-923. Doi:
793 10.1126/science.297.5583.920.
794 Mayer, L.M., 1994. Surface area control of organic carbon accumulation in continental
795 shelf sediments. Geochim. Cosmochim. Acta 58, 1271-1284. Doi: 10.1016/0016-
796 7037(94)90381-6.

797 Mendes, L.A., de Lena, J.C., do Valle, C.M., Fleming, P.M., Windmöller, C.C., 2016.
798 Quantification of methylmercury and geochemistry of mercury in sediments from
799 a contaminated area of Descoberto (MG), Brazil. Appl. Geochem. 75, 32-43. Doi:
800 10.1016/j.apgeochem.2016.10.011.
801 Moncur, M.C., Ptacek, C.J., Lindsay, M.B.J., Blowes, D.W., Jambor, J.L., 2015. Long-
802 term mineralogical and geochemical evolution of sulfide mine tailings under a
803 shallow water cover. Appl. Geochem. 57, 178-193. Doi: DOI
804 10.1016/j.apgeochem.2015.01.012.
805 Mulligan, C.N., Yong, R.N., Gibbs, B.F., 2001. Remediation technologies for metal-
806 contaminated soils and groundwater: an evaluation. Eng. Geol. 60, 193-207. Doi:
807 10.1016/s0013-7952(00)00101-0.
808 Muyzer, G., Stams, A.J.M., 2008. The ecology and biotechnology of sulphate-reducing
809 bacteria. Nat. Rev. Microbiol. 6, 441-454. Doi: 10.1038/nrmicro1892.
810 Nordstrom, D.K., 1977. Thermochemical redox equilibria of ZoBell's solution. Geochim.
811 Cosmochim. Acta 41, 1835-1841. Doi: 10.1016/0016-7037(77)90215-0.
812 Noyce, G.L., Basiliko, N., Fulthorpe, R., Sackett, T.E., Thomas, S.C., 2015. Soil
813 microbial responses over 2 years following biochar addition to a north temperate
814 forest. Biol. Fertil. Soils 51, 649-659. Doi: 10.1007/s00374-015-1010-7.
815 Oak Ridge National Laboratory, 2015. Predicted mercury methylators.
816 http://www.esd.ornl.gov/programs/rsfa/data/PredictedMethylators/PredictedMeth
817 ylators_20140514.pdf (Accessed by November 30, 2015),
818 Ortiz, V.L., Mason, R.P., Ward, J.E., 2015. An examination of the factors influencing
819 mercury and methylmercury particulate distributions, methylation and
820 demethylation rates in laboratory-generated marine snow. Mar. Chem. 177, 753-
821 762. Doi: 10.1016/j.marchem.2015.07.006.
822 Patmont, C.R., Ghosh, U., LaRosa, P., Menzie, C.A., Luthy, R.G., Greenberg, M.S.,
823 Cornelissen, G., Eek, E., Collins, J., Hull, J., Hjartland, T., Glaza, E., Bleiler, J.,
824 Quadrini, J., 2015. *In situ* sediment treatment using activated carbon: a
825 demonstrated sediment cleanup technology. Integr. Environ. Assess. Manag. 11,
826 195-207. Doi: 10.1002/ieam.1589.
827 Paulson, K.M.A., Ptacek, C.J., Blowes, D.W., Gould, W.D., Ma, J., Landis, R.C., Dyer,
828 J.A., 2016. Role of organic carbon sources and sulfate in controlling net
829 methylmercury production in riverbank sediments of the South River, VA (USA).
830 Geomicrobiol. J., 1-14. Doi: 10.1080/01490451.2016.1247483.
831 Pereira, M.E., Duarte, A.C., Millward, G.E., Vale, C., Abreu, S.N., 1998. Tidal export of
832 particulate mercury from the most contaminated area of Aveiro's Lagoon,
833 Portugal. Sci. Total Environ. 213, 157-163. Doi: 10.1016/S0048-9697(98)00087-
834 4.
835 Poissant, L., Pilote, M., 1998. Mercury concentrations in single event precipitation in
836 southern Québec. Sci. Total Environ. 213, 65-72. Doi: 10.1016/S0048-
837 9697(98)00076-X.
838 Randall, P.M., Chattopadhyay, S., 2013. Mercury contaminated sediment sites-an
839 evaluation of remedial options. Environ. Res. 125, 131-149. Doi:
840 10.1016/j.envres.2013.01.007.

841 Ribet, I., Ptacek, C.J., Blowes, D.W., Jambor, J.L., 1995. The potential for metal release
842 by reductive dissolution of weathered mine tailings. J. Contam. Hydrol. 17, 239-
843 273. Doi: 10.1016/0169-7722(94)00010-F.
844 Riedel, T., Iden, S., Geilich, J., Wiedner, K., Durner, W., Biester, H., 2014. Changes in
845 the molecular composition of organic matter leached from an agricultural topsoil
846 following addition of biomass-derived black carbon (biochar). Org. Geochem. 69,
847 52-60. Doi: 10.1016/j.orggeochem.2014.02.003.
848 Rondon, M.R., Goodman, R.M., Handelsman, J., 1999. The Earth's bounty: assessing and
849 accessing soil microbial diversity. Trends Biotechnol. 17, 403-409. Doi:
850 10.1016/S0167-7799(99)01352-9.
851 Serrano, S., Vlassopoulos, D., Bessinger, B., O'Day, P.A., 2012. Immobilization of Hg(II)
852 by coprecipitation in sulfate-cement systems. Environ. Sci. Technol. 46, 6767-
853 6775. Doi: 10.1021/es202939v.
854 Serrano, S., Vlassopoulos, D., O'Day, P.A., 2016. Mechanism of Hg(II) immobilization
855 in sediments by sulfate-cement amendment. Appl. Geochem. 67, 68-80. Doi:
856 10.1016/j.apgeochem.2016.01.007.
857 Shackley, S., Ruysschaert, G., Zwart, K., Glaser, B., 2016. Biochar in European Soils and
858 Agriculture: Science and Practice. Taylor & Francis, Abingdon, Oxon, United
859 Kingdom.
860 Shu, R., Wang, Y., Zhong, H., 2016. Biochar amendment reduced methylmercury
861 accumulation in rice plants. J. Hazard. Mater. 313, 1-8. Doi:
862 10.1016/j.jhazmat.2016.03.080.
863 Silverstein, R.M., Bassler, G.C., Morrill, T.C., 1974. Spectrometric Identification of
864 Organic Compounds, 3rd ed. John Wiley & Sons, New York.
865 Spokas, K.A., 2010. Review of the stability of biochar in soils: predictability of O:C
866 molar ratios. Carbon Manag. 1, 289-303. Doi: 0.4155/CMT.10.32.
867 Spokas, K.A., Novak, J.M., Masiello, C.A., Johnson, M.G., Colosky, E.C., Ippolito, J.A.,
868 Trigo, C., 2014. Physical disintegration of biochar: an overlooked process.
869 Environ. Sci. Technol. Lett. 1, 326-332. Doi: 10.1021/ez500199t.
870 Stordal, M., Gill, G., Wen, L.S., Santschi, P., 1996. Mercury phase speciation in the
871 surface waters of three Texas estuaries: importance of colloidal forms. Limnol.
872 Oceanogr. 41, 52-61.
873 Tchounwou, P.B., Ayensu, W.K., Ninashvili, N., Sutton, D., 2003. Environmental
874 exposure to mercury and its toxicopathologic implications for public health.
875 Environ. Toxicol. 18, 149-175. Doi: 10.1002/tox.10116.
876 Uchimiya, M., Ohno, T., He, Z., 2013. Pyrolysis temperature-dependent release of
877 dissolved organic carbon from plant, manure, and biorefinery wastes. J. Anal.
878 Appl. Pyrol. 104, 84-94. Doi: 10.1016/j.jaap.2013.09.003.
879 Ullrich, S.M., Tanton, T.W., Abdrashitova, S.A., 2001. Mercury in the aquatic
880 environment: a review of factors affecting methylation. Crit. Rev. Environ. Sci.
881 Technol. 31, 241-293. Doi: 10.1080/20016491089226.
882 US EPA, 2002. Method 1631: Revision E: mercury in water by oxidation, purge and trap,
883 and cold vapor atomic fluorescence spectrometry, Washington DC, USA.
884 Wang, J., Feng, X., Anderson, C.W.N., Xing, Y., Shang, L., 2012. Remediation of
885 mercury contaminated sites - A review. J. Hazard. Mater. 221-222, 1-18. Doi:
886 10.1016/j.jhazmat.2012.04.035.

887 Weisener, C.G., Sale, K.S., Smyth, D.J.A., Blowes, D.W., 2005. Field column study
888 using zerovalent iron for mercury removal from contaminated groundwater.
889 Environ. Sci. Technol. 39, 6306-6312. Doi: 10.1021/es050092y.
890 Weishaar, J.L., Aiken, G.R., Bergamaschi, B.A., Fram, M.S., Fujii, R., Mopper, K., 2003.
891 Evaluation of specific ultraviolet absorbance as an indicator of the chemical
892 composition and reactivity of dissolved organic carbon. Environ. Sci. Technol. 37,
893 4702-4708. Doi: 10.1021/es030360x.
894 Yu, R., Flanders, J.R., Mack, E.E., Turner, R., Mirza, M.B., Barkay, T., 2011.
895 Contribution of coexisting sulfate and iron reducing bacteria to methylmercury
896 production in freshwater river sediments. Environ. Sci. Technol. 46, 2684–2691.
897 Doi: 10.1021/es2033718.
898 Yu, R.Q., Reinfelder, J.R., Hines, M.E., Barkay, T., 2013. Mercury methylation by the
899 methanogen *Methanospirillum hungatei*. Appl. Environ. Microbiol. 79, 6325-
900 6330. Doi: 10.1128/AEM.01556-13.
901 Yudovich, Y.E., Ketris, M.P., 2005. Mercury in coal: a review. Part 1. Geochemistry. Int.
902 J. Coal Geol. 62, 107-134. Doi: 10.1016/j.coal.2004.11.002.
903 Zhang, Y., Liu, Y.-R., Lei, P., Wang, Y.-J., Zhong, H., 2018. Biochar and nitrate reduce
904 risk of methylmercury in soils under straw amendment. Sci. Total Environ. 619,
905 384-390.
906 Zhong, S., Qiu, G., Feng, X., Lin, C., Bishop, K., 2018. Sulfur and iron influence the
907 transformation and accumulation of mercury and methylmercury in the soil-rice
908 system. J. Soils Sediments 18, 578-585. Doi: 10.1007/s11368-017-1786-1.
909

910

911 Table 1. Properties, elemental composition, and released component from activated
912 carbon (AC), Cowboy Charcoal (OAK700), low-T (GRASS300) and high-T (GRASS600)
913 switchgrass, and high-T poultry manure (MANURE600) biochars

Element	AC	OAK700	GRASS300[a]	GRASS600[a]	MANURE600
Specific surface area, $m^2\ g^{-1}$	600	65	2.6	230	5.2
C, %	98.0±0.8	99.9±0.6	70.2±1.7	94.5±1.4	18.5±1.4
S, %	0.18±0.01	<0.01	0.10±0.01	0.55±0.02	0.48±0.02
Ag, $\mu g\ g^{-1}$	< 0.01	< 0.01	0.06	0.87	0.16
Al, $\mu g\ g^{-1}$	1400	45	160	240	14000
Ar, $\mu g\ g^{-1}$	< 0.5	< 0.5	< 0.5	< 0.5	1.9
Ba, $\mu g\ g^{-1}$	59	67	22	37	200
Be, $\mu g\ g^{-1}$	0.09	0.02	< 0.02	< 0.02	0.60
Bi, $\mu g\ g^{-1}$	< 0.09	< 0.09	< 0.09	< 0.09	< 0.09
Ca, $\mu g\ g^{-1}$	7200	2900	9200	14000	44000
Cd, $\mu g\ g^{-1}$	< 0.02	< 0.02	0.03	< 0.02	1.2
Co, $\mu g\ g^{-1}$	0.51	0.63	0.16	0.21	3.5
Cr, $\mu g\ g^{-1}$	4.3	1.2	3.4	5.4	27
Cu, $\mu g\ g^{-1}$	9.1	4.5	7.2	12	34
Fe, $\mu g\ g^{-1}$	1700	13	2100	1700	10000
K, $\mu g\ g^{-1}$	910	2600	9300	11000	28000
Li, $\mu g\ g^{-1}$	< 2	< 2	< 2	< 2	9
Mg, $\mu g\ g^{-1}$	4200	690	2100	3500	7700
Mn, $\mu g\ g^{-1}$	110	120	210	260	250
Mo, $\mu g\ g^{-1}$	0.4	< 0.1	0.2	0.4	7.1
Na, $\mu g\ g^{-1}$	910	5.2	18	29	17000
Ni, $\mu g\ g^{-1}$	1.7	2.7	0.6	1.2	8.4
P, $\mu g\ g^{-1}$	890	110	930	1600	14000
Pb, $\mu g\ g^{-1}$	0.08	1.2	0.47	1.2	140
Sb, $\mu g\ g^{-1}$	< 0.8	< 0.8	< 0.8	< 0.8	< 0.8
Se, $\mu g\ g^{-1}$	1.4	< 0.7	< 0.7	< 0.7	1.7
Sn, $\mu g\ g^{-1}$	0.6	< 0.5	7.0	130	4.5
Sr, $\mu g\ g^{-1}$	60	17	18	30	180
Ti, $\mu g\ g^{-1}$	98	1.5	11	27	1800
TI, $\mu g\ g^{-1}$	< 0.02	< 0.02	< 0.02	< 0.02	0.12
U, $\mu g\ g^{-1}$	0.19	0.006	0.008	0.012	1.2
V, $\mu g\ g^{-1}$	10	< 1	< 1	< 1	21
Y, $\mu g\ g^{-1}$	0.69	0.39	0.38	0.39	7.6
Zn, $\mu g\ g^{-1}$	1.8	7.8	23	35	330
pH[b]	10	8.0	8.4	9.9	11
Alkalinity[b], $mg\ g^{-1}$	4.4	5.3	7.7	11.3	6.6
OA[b], $mg\ g^{-1}$	0.03	0.05	0.14	0.11	0.11
DOC[b], $mg\ g^{-1}$	0.11	0.41	0.98	0.16	<0.003

914 [a] data from Liu et al. (2017)
915 [b] pH value measured in river water reacted with biochar for 48 hr using a 1:75 biochar to
916 water mass ratio as reported in Liu et al. (2015); other values obtained similarly but
917 expressed per g biochar

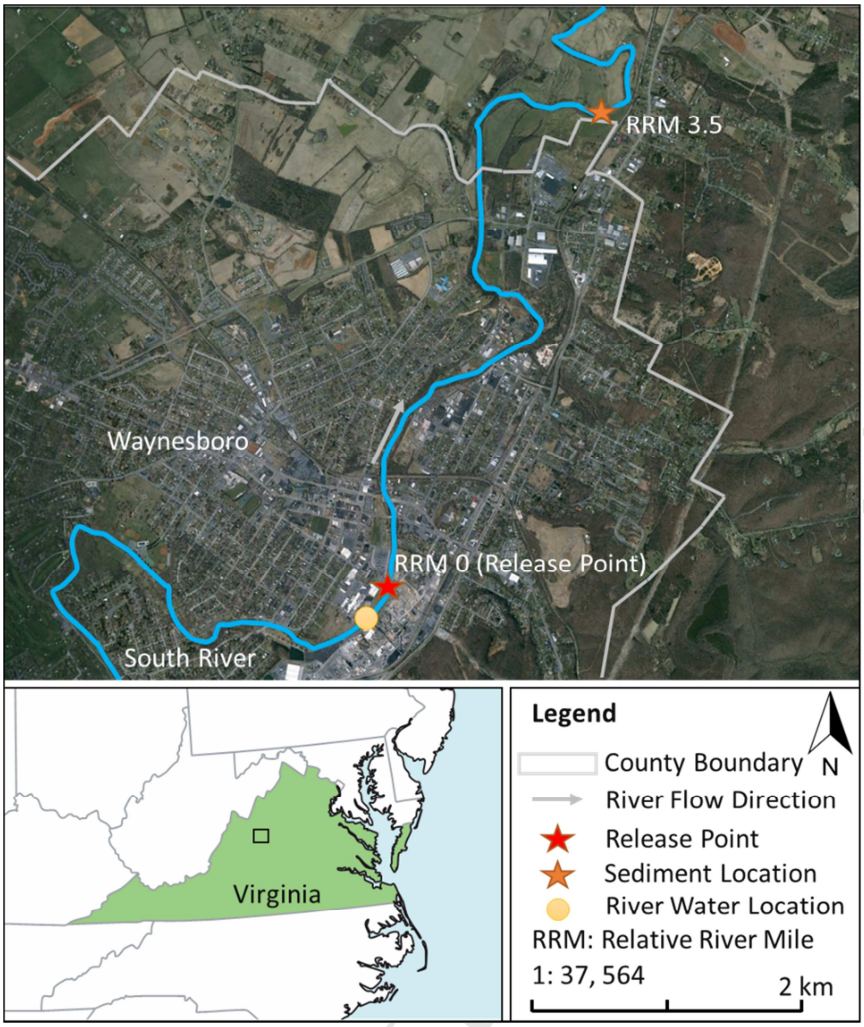

Figure 1. Sampling locations for sediment (orange star) and river water (orange circle) used in this study.

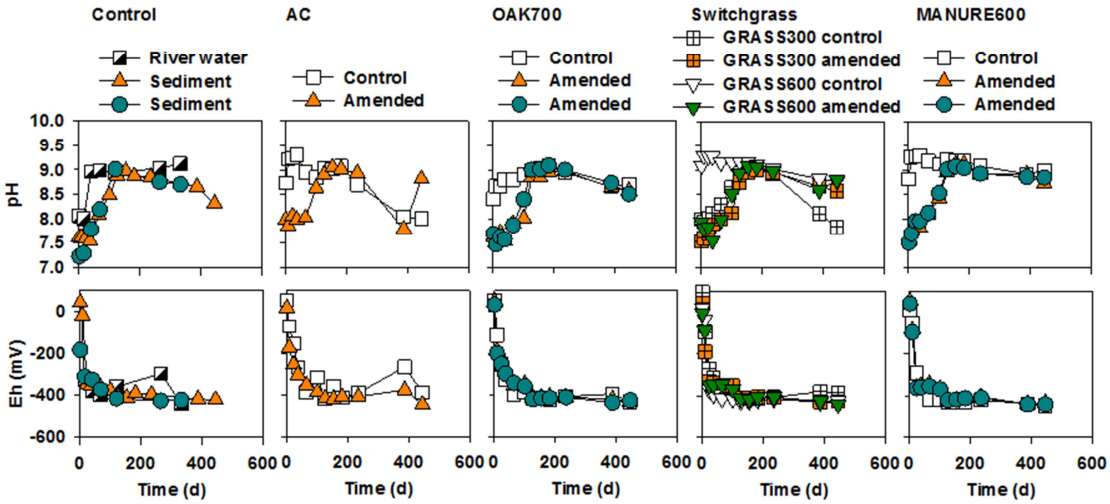

Figure 2. pH and Eh values of control and amended systems vs. time.

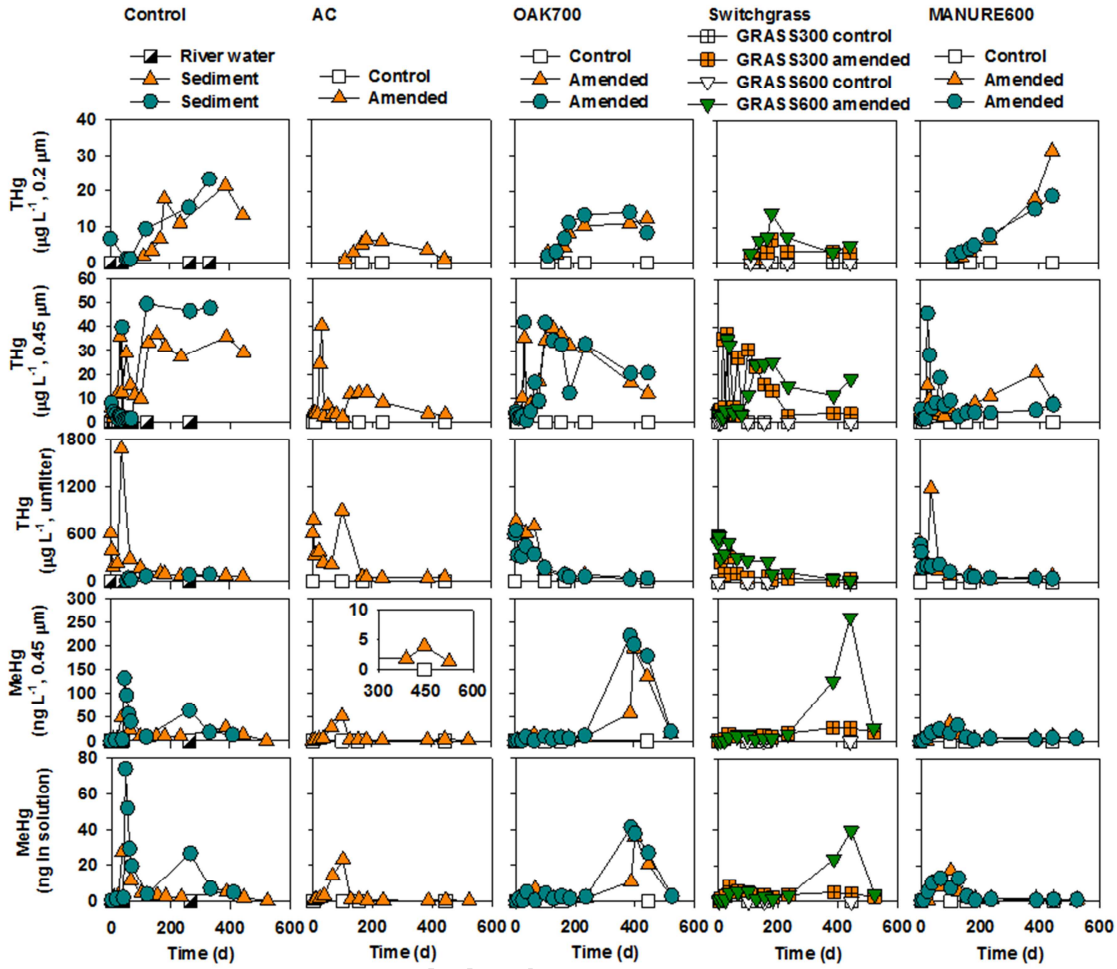

Figure 3. Concentrations of 0.2- and 0.45-µm filtered THg and 0.45-µm filtered MeHg in aqueous solutions of control and amended systems vs. time. Sediment control and low-T and high-T switchgrass biochar data are from Liu et al. (2017).

1

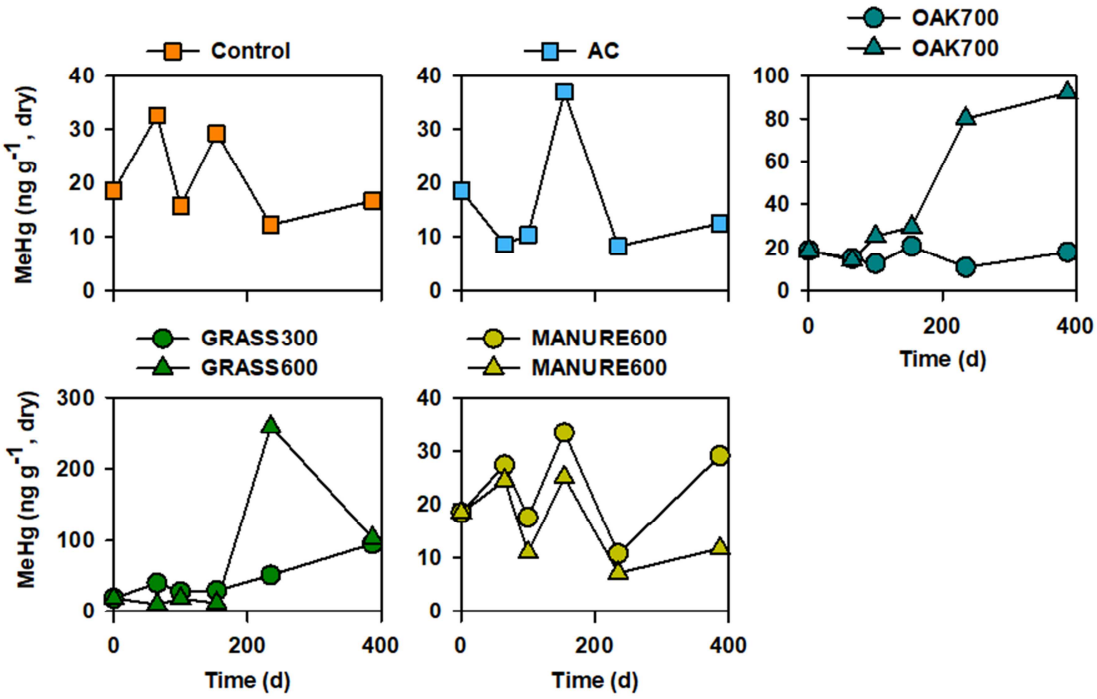

2

3 Figure 4. MeHg content in sediment control and amended systems (activated carbon,
4 OAK700, low-T and high-T switchgrass, and poultry manure) vs. time. Sediment control
5 and low-T and high-T switchgrass biochar data are from Liu et al. (2017). Note: change
6 in y-axis scale for different subplots.
7
8

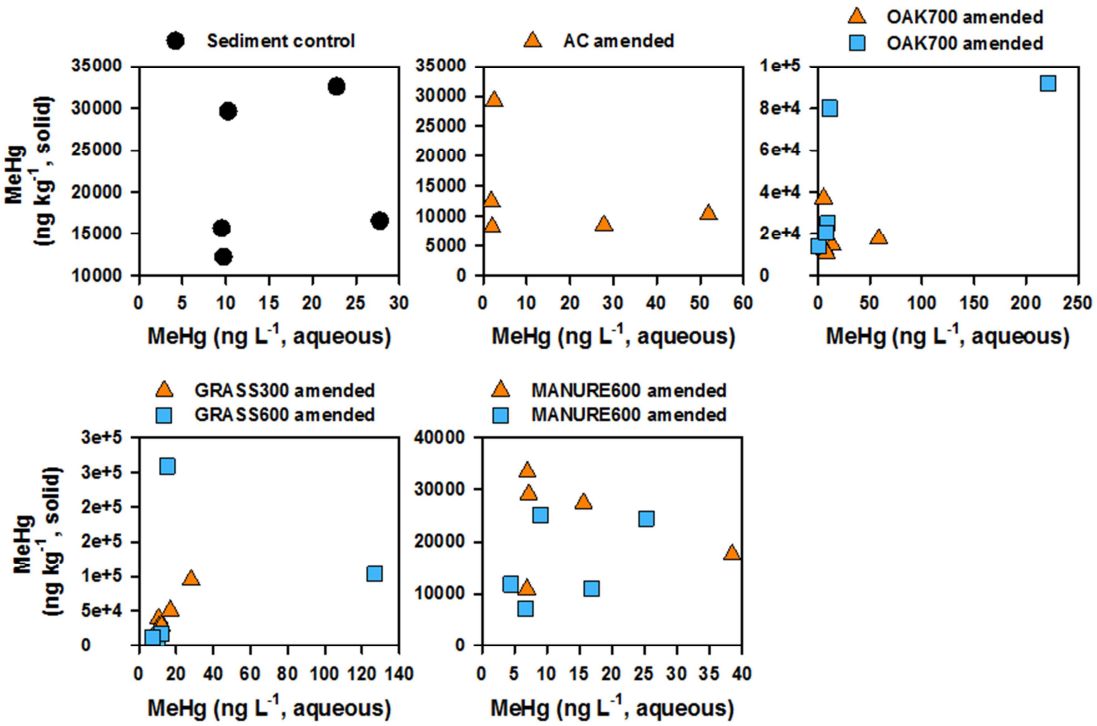

Figure 5. Aqueous phase MeHg concentrations vs. solid phase MeHg content of sediment control and amended systems.

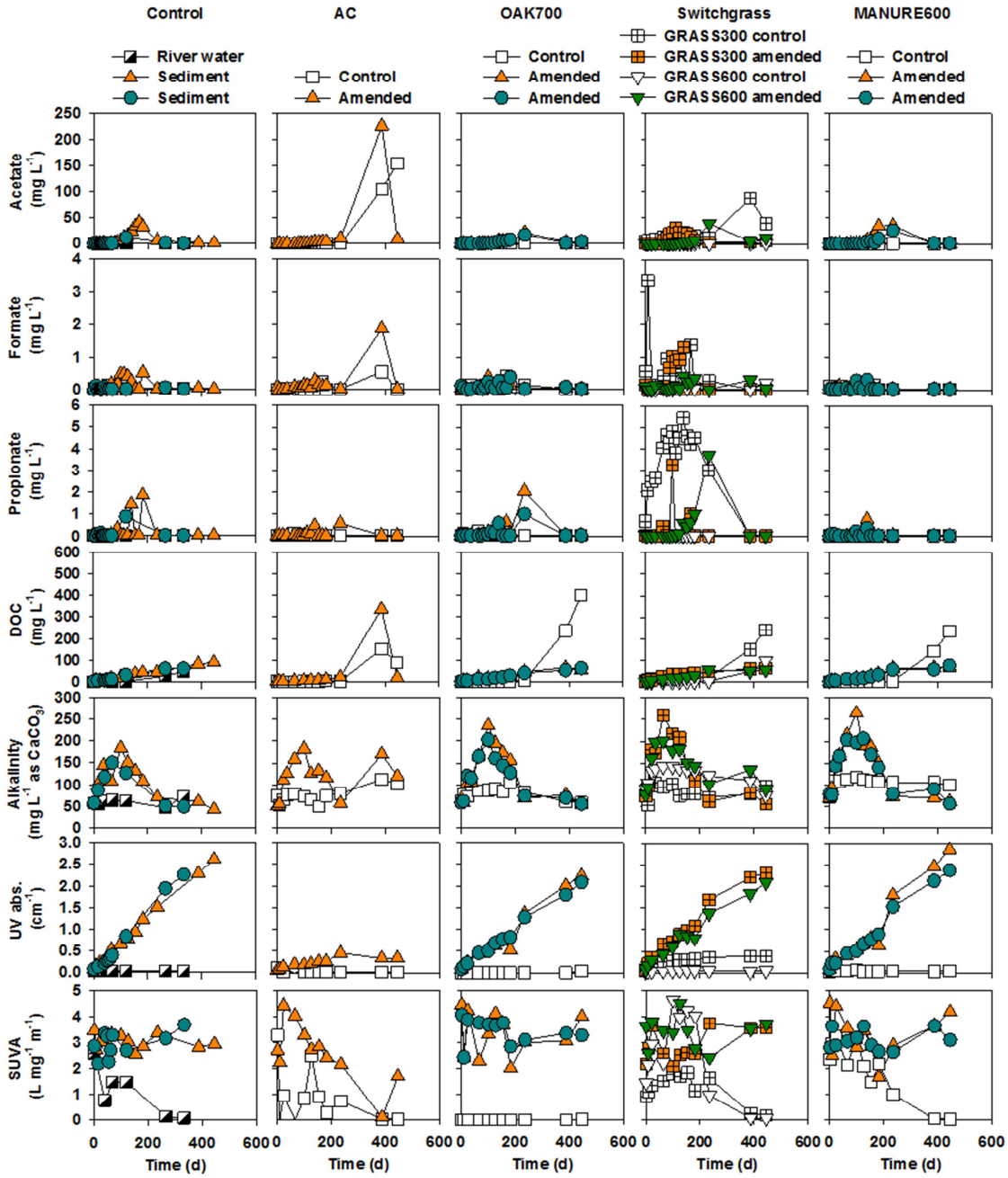

Figure 6. Concentrations of carbon sources (acetate, formate, propionate, DOC, and alkalinity), UV absorbance at 254 nm, and calculated SUVA in aqueous solutions of control and amended systems vs. time. Sediment control and low-T and high-T switchgrass biochar data are from Liu et al. (2017).

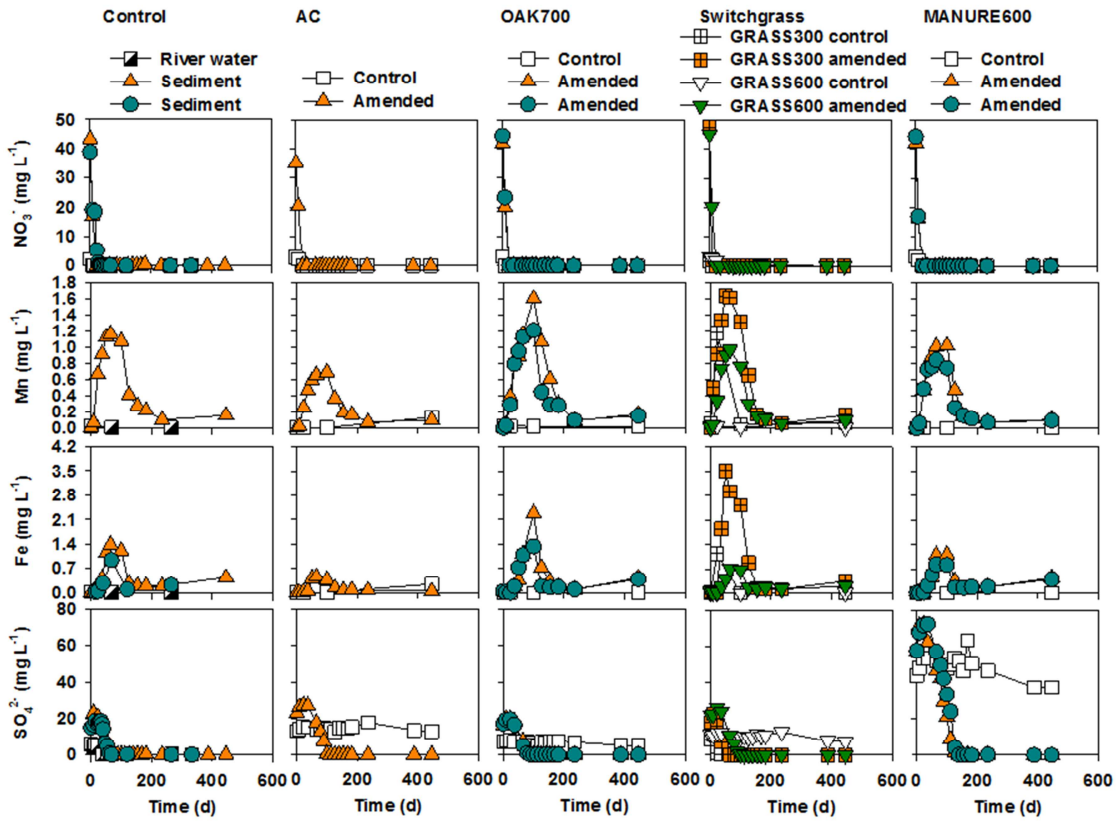

Figure 7. Concentrations of electron acceptors (NO_3^-, Mn, Fe, and SO_4^{2-} in redox sequence) in aqueous solutions of control and amended systems vs. time. Fe and SO_4^{2-} concentrations of sediment control and low-T and high-T switchgrass biochar data are from Liu et al. (2017).

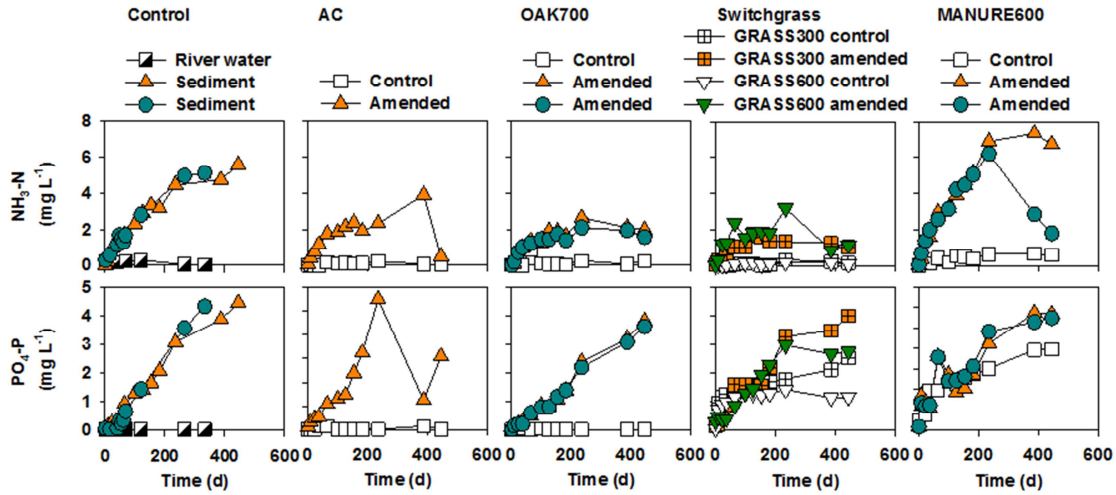

Figure 8. Concentrations of nutrients (NH_3-N and PO_4-P) in aqueous solutions of control and amended systems vs. time.

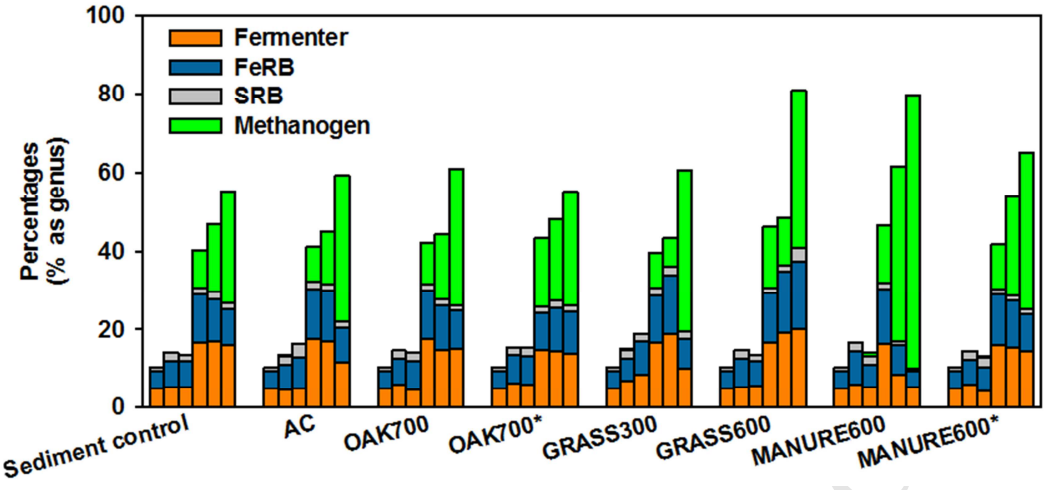

Figure 9. Pyrosequencing results as percentages in genus level, including fermenters, FeRB, SRB, and methanogens of sediment control and activated carbon, OAK700 (duplicate), low-T and high-T switchgrass biochar, and poultry manure biochar (duplicate) amended systems. For each sample, columns from left to right represent days 0, 65, 100, 154, 235, and 387, respectively. Sediment control and low-T and high-T switchgrass biochar data are from Liu et al. (2017).

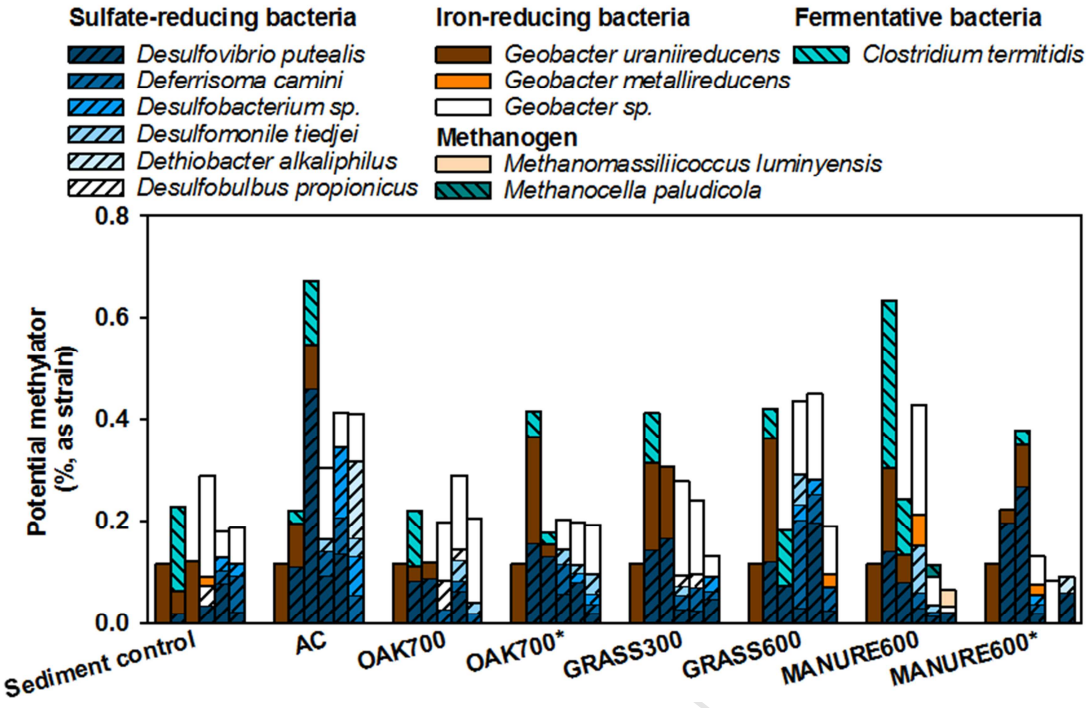

Figure 10. Percentages of species identified as known Hg methylators, including SRB, FeRB, methanogen, and fermentative bacteria, for different days from sediment control and amended systems. For each sample, columns from left to right represent day 0, 65, 100, 154, 235, and 387, respectively. Sediment control and low-T and high-T switchgrass biochar data are from Liu et al. (2017).

- Total Hg is under control using biochar after certain period
- MeHg concentration in amended systems is generally lower than in sediment control
- MeHg change corresponds to onset of Fe and SO_4^{2-} reduction and methanogenic stages
- Switchgrass biochar pyrolyzed at 300^{o}C is the most promising reactive medium